Optimization of Multiple Wells in Carbon Sequestration

by

Swathi Gangadharan

A thesis
presented to the University of Waterloo
in fulfillment of the
thesis requirement for the degree of
Master of Applied Science
in
Chemical Engineering

Waterloo, Ontario, Canada, 2014

I hereby declare that I am the sole author of this thesis. This is a true copy of the thesis, including any required final revisions, as accepted by my examiners.

I understand that my thesis may be made electronically available to the public.

Abstract

Injection of CO_2 in saline aquifers is considered as one of the best strategies for the reduction of greenhouse gases. In order to select a potential saline aquifer storage site for carbon sequestration, many parameters are considered such as relative permeability, thickness, compressibility, porosity, salinity and well interference. These are significant because they affect the CO_2 storage capacity of the reservoir. The one of the most important criteria to be considered during sequestration is the pressure profile inside the reservoir as the sequestered CO_2 increases the pressure within the saline formation over time. In order to maintain the integrity of the reservoir, the reservoir pressure is always maintained below the fracture pressure. Thus, modeling of pressure profile is essential as it controls the maximum amount of CO_2 which can be into the reservoir. There are various analytical and numerical models to determine the bottom-hole pressure for CO_2 injection.

The main objective of my thesis is to examine and identify the analytical approaches in modeling of pressure profile during CO_2 injection. It includes single injection as well as multiple wells injection scenarios. The second case is much more important from practical point of view and applicability of analytical tools should be validated. Two models of injection/production are considered: (i) Single-phase (brine production from a brine reservoir) and (ii) Two phase model (CO_2 injection in a brine reservoir). In both cases, we analyzed the pressure build-up and discussed the results in comparison with numerical simulations. We also present a sensitivity analysis of the reservoir parameters on CO_2 sequestration.

The second part of the thesis focuses on finding ways to increase the CO_2 injection capacity of saline aquifers by using the technique of multiple wells injection strategy. Numerous test cases will be presented to optimize the well placement and number of wells to get the maximum sequestration. The thesis will look upon the different ways to maintain the reservoir pressure below fracture pressure such as optimization of injection wells, varying the flow-rates of injection wells and by placement of relief wells to produce brine from the reservoir.

Acknowledgements

First and foremost, I would like to thank God for without Him any of this would not be possible. All praises and accolades go to Him.

I would like to express my deep gratitude and sincere appreciation to my supervisor Dr. Yuri Leonenko for his support, encouragement and guidance throughout my masters thesis. I am especially grateful to Yuri for giving me masters when I really needed. He has been also a consistent source of knowledge and inspiration. It was a distinct privilege for me to work with him.

I would also like to thank my thesis readers Dr. Ali Elkamel and Dr. Marios Ioannidis for having the patience and taking the time to read this thesis, and provide useful comments and suggestions.

I would like to acknowledge Joshi for his help in adapting to some of the modeling presented in this work. I would also like to thank Dr. Amin for being extremely supportive of me working under him in water treatment paper. Another enormously positive impact of my life has been my two years at Waterloo with two wonderful friends, Akash and Srinivasan. They have been a great source of strength and support for me through each step in Waterloo. A big Thank you for being there for me.

I would also like to thank my roommates, Yu and Tracy for all the badminton times and my friends Ankita, Preetam, Mani, Bhushan, Ushnik, Manoj, Sami for their support and friendship.

Lastly, and most importantly, I have to thank my Mom, Dad and Brother for their love, encouragement and utmost faith in me and my ability to achieve my highest potential.

Dedication

I dedicate this thesis to Mumma, Papa and Bro, Swaroop who supported me through each step in the way.

Table of Contents

List of Tables

List of Figures

Nomenclature

B_w	Brine Formation volume factor [res m^3/std m^3]
B_g	Gas formation volume factor [res m^3/std m^3]
B	Thickness of formation [m]
$b(r)$	Thickness of the CO_2 layer [m]
λ	Total mobility, dimensionless
c_g	Gas compressibility $[Pa^{-1}]$
c_r	Rock compressibility $[Pa^{-1}]$
c_w	Water compressibility $[Pa^{-1}]$
c_t	Total compressibility $[S_g c_g +$ (1-S_g)c_w+$c_r][Pa^{-1}]$
c_{tg}	Total compressibility of gas region $[c_g$+$c_r][Pa^{-1}]$
c_{tw}	Total compressibility of brine region $[c_w$+$c_r]$ $[Pa^{-1}]$
D_{BL-dry}	Retardation factor for drying front, dimensionless
$D_{brine-BL}$	Retardation factor for two-phase front, dimensionless
Ei	Exponential integral function
f_g	Fractional flow of gas, dimensionless
$F_{\lambda g}$	Total mobility $[\lambda_g$+$\lambda_w/\bar{\lambda_g}]$ dimensionless
$F_{\lambda w}$	Total mobility $[\lambda_g$+$\lambda_w/\bar{\lambda_w}]$ dimensionless
h	Formation thickness [m]
m	Corey Gas Exponent
n	Corey Brine Exponent
$\omega_{CO_2,a}$	Mole fraction of CO_2 in brine phase
$\omega_{Brine,a}$	Mole fraction of Brine in CO_2 phase
ρ_{aD}	Molar density [kg/m^3]
k	Permeability $[m^2]$
k^0_{rg}	Gas Endpoint relative permeability, dimensionless
k_{rg}	Gas relative permeability, dimensionless
$\bar{k}_{rg}$	Gas relative permeability in gas zone, dimensionless
k_{rw}	Brine relative permeability, dimensionless
$\bar{k}_{rw}$	Brine relative permeability in brine zone, dimensionless
η_{D2}	Diffusivity ratio $[c_{tg}/c_t]$ dimensionless
η_{D3}	Diffusivity ratio $[(c_{tg}/c_{tw})(\bar{\lambda_w}/\bar{\lambda_g})]$ dimensionless
P_D	Dimensionless pressure [Pa]
P_i	Initial pressure [Pa]
P_f	Formation fracture pressure [Pa]
ϕ	Porosity
λ_g	Gas Mobility $[\frac{k_{rg}}{\mu_g}]$

λ_w	Brine Mobility $[\frac{k_{rw}}{\mu_w}]$
$\bar{\lambda}_g$	Gas Mobility in gas zone $[\frac{\bar{k}_{rg}}{\mu_g}]$
$\bar{\lambda}_w$	Brine Mobility in brine zone $[\frac{\bar{k}_{rw}}{\mu_w}]$
μ_g	CO_2 Viscosity [Pa.s]
μ_w	Brine Viscosity [Pa.s]
q	Gas injection rate $[m^3/\text{s}]$
r	Radius of well [m]
r_e	Formation external boundary radius [m]
r_D	Dimensionless radius $[\frac{r}{r_w}]$
r_w	Wellbore radius [m]
r_{dry}	Radial position of drying-out zone [m]
r_{DBL}	Radial position of two phase zone [m]
x_w	X coordinate of the well [m]
y_w	Y coordinate of the well [m]
S_g	Gas saturation
S_{gBL}	Gas saturation of BL front
S_{gdry}	Gas saturation of Dry front
$S_{g,ave}$	Average gas saturation $[\frac{S_{gBL}+S_{gdry}}{2}]$
t	Time [s]
t_D	Dimensionless time $[\frac{kk_{rg}}{\mu_g \phi r_w^2 c_{tg}}]$
ϵ	Dimensionless $[\frac{qc_{tg}\mu_g}{4\pi hkk_{rg}B_g}]$

List of Acronyms

CO_2	Carbon Dioxide
CH_4	Methane
N_2O	Nitrous Oxide
SF_6	Sulphur Hexafluoride
ppm	Parts per million
Pa	Pascal
MPa	MegaPascal
Gt	Gigatones
Mt	Megatones
kt	Kilotones
Pt	Petagram
mD	Millidarcy
m	Meter
km	Kilometer
cP	Centipoise
rB	Reservoir Barrels

SCF	Standard cubic feet
psi	Pounds per square inch
s	Second
$IPCC$	Intergovernmental Panel on Climate Change
CMG	Computer Modelling Group
$3D$	Three Dimensional Plot
GHG	Greenhouse Gas
BHP	Bottom-hole pressure
BL	Buckley-Leverett model

Chapter 1

Introduction

It is widely accepted that emissions from fossil fuels for electricity production and industrial processes are one of the major contributors to global warming. These emissions greatly increase the concentration of greenhouse gases (GHG) in the atmosphere. The most significant of these GHGs which affect the environment are CO_2, CH_4, N_2O, hydrofluorocarbons and SF_6. Among this gases, CO_2 is considered as one of the most prevalent GHG in the atmosphere. According to the 2010 assessment report by the Intergovernmental Panel on Climate Change (IPCC), the observed global warming over last 50 years is due to the rise in atmospheric concentration of CO_2. If no serious action is taken, the concentration of CO_2 will reach to about 500ppm within next 50 years with an annual increase rate of about 2ppm [1, 2]. The average global temperature has increased from $0.6 \pm 0.2\,^{\circ}\mathrm{C}$ since the nineteen century and it is predicted to increase by 1.4 to $5.8\,^{\circ}\mathrm{C}$ by 2100 as shown in Figure 1.1. There are various drastic effects of global warming such as rise in sea levels, increased frequency of floods and droughts and climate perturbations.

As the world population is growing so is the global energy demand. According to the IPCC report in 2010 [1], it is estimated that the global energy demand will increase by about 35% from 2010 to 2040. Thus, to meet this rise in demand, we will need a diverse, reliable and affordable fuel mix so as to enable the economic growth and societal advancements. Fossil fuels like oil, natural gas and coal will remain dominant energy resource for the next decades and will continue to attract large fraction of global energy demand *i.e.* about 80% of total global energy by 2040. Thus, there is a need for development of energy efficient technologies with low or no CO_2 footprint so as to mitigate the rise in CO_2 concentration into the atmosphere. Now, the question is whether these energy efficient technologies will emit less or no CO_2? Today, all the CO_2 emissions resulted due to the combustion of fossil fuels is emitted into the atmosphere and we have been doing this since

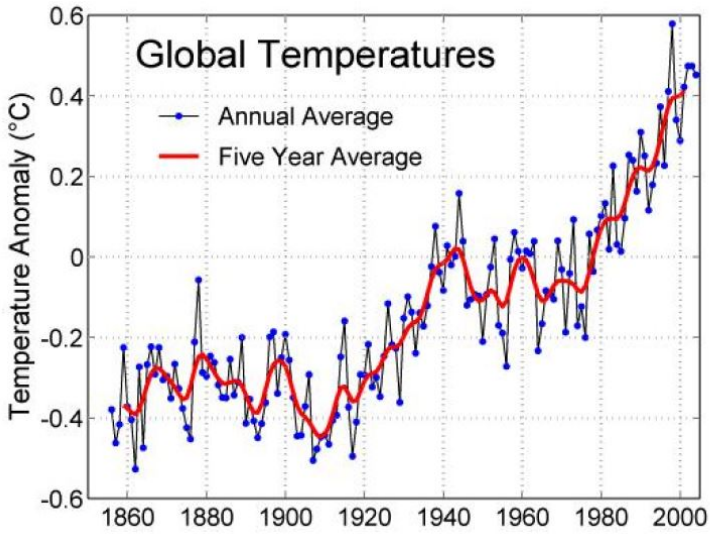

Figure 1.1: [1] Recorded Global temperature according to IPCC report.

50 years because we believed it was not harmful. There have been many technologies implemented to treat various other emissions as cited in [2] such as how a sewage treatment plants are used to remove pathogens from lakes and also how SF_6 and N_2O are removed from power plants and industrial process. However, there has been big challenge to reduce CO_2 emissions from fossil fuel combustion at low cost. There are many technologies to reduce the CO_2 emissions into the atmosphere such as energy decarbonization, increasing renewable and nuclear energy generation, enhancing carbon sinks and Carbon Capture and Storage (CCS).

Carbon Capture and Storage (CCS) is considered to be one of the promising option for reducing CO_2 emissions from power and industrial sectors. It is considered as an emerging transition technology which provides a solution for a long-term storage of CO_2. CCS is the process in which CO_2 is captured from the emission source, transported it to a storage location and stored underground that ensures long-term isolation from the atmosphere. The main aim in CCS is to allow the use of fossil fuels while reducing CO_2 emissions, thereby mitigating climate change as shown in Figure 1.2. According to IPCC 2010 report [1], it was reported that power plant with CCS could reduce CO_2 emissions by 80-90% when compared to power plants without CCS.

Geological sequestration is considered as a viable and an acceptable option for CO_2 storage because of their availability, high storage capacity and the ability to lock down CO_2

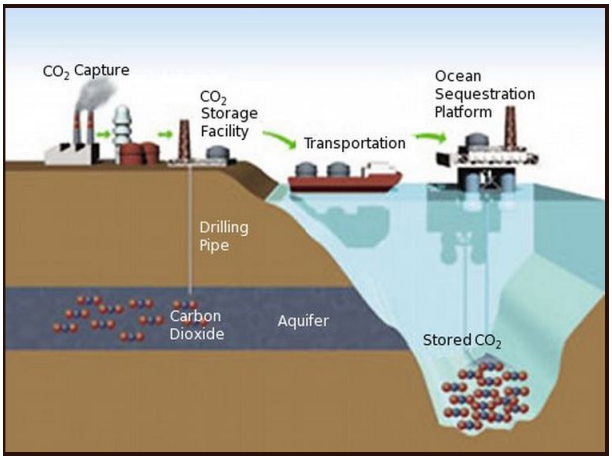

Figure 1.2: [3] Options of CCS.

permanently back into the ground. There are number of ways to sequester in geological structures and their detailed description are presented in the Section 2:

- Depleted Oil & Gas Reservoirs,
- Depleted Coal Seams,
- Deep Underground Aquifers,
- Deep Ocean Sequestration.

Among the sequestration options mentioned above, this thesis restricts it analysis and discussion to CO_2 storage in deep water (brine) formations (aquifers or saline aquifers). CO_2 storage in aquifers has drawn in a lot of attention recently due to high storage capacity, confinement and injectivity. Sequestration in geological formations has less environmental problems when compared to ocean sequestration, the latter leading to ocean acidification. Thus, CO_2 sequestration in aquifer is safely undertaken and practiced. In order to make carbon sequestration in saline formations a viable option to tackle climate change, we should be able to sequester large quantities of CO_2 on a scale of billion of metric tons (Gigaton) per year. Presently, all the four major CCS projects are injecting at the rate of 1 Megaton (Mt) per year (Table 1.1). Recent report [1] have suggested that deep saline formation have a storage capacity of around 2000 Gigatons of CO_2 which are two orders of magnitude higher than the total worldwide emissions, making it practical potential storage option.

Project	**Leader**	**Location**	CO_2 **Sink**
Sleipner (1996)	Statoil	North Sea, Norway	Saline formation
Weyburn (2000)	Pan Canadian	Saskatchewan, Canada	Enhanced Oil Recovery
In Salah (2004)	British Petroleum	Algeria	Gas Reservoir
Snohvit (2008)	Statoil	Barents Sea, Norway	Saline formation

Table 1.1: [3] Major CCS Projects in Operation.

One of our main purposes is to examine options in maximizing storage capacity of the reservoir. And here we are talking about injection capacity: how much can be injected within a short period of time (50 years and within limited injection area). Injection capacity could be much lower than one defined by available pore space. To fill the pore space, substantial time is needed to avoid reaching fracture pressure. It becomes very important when large volume is to be injected (scales of 10 Mt/year, which is order of magnitude higher than currently achieved in the projects mentioned above). In order to maintain the integrity of the reservoir, it is really important to understand how much a reservoir can store CO_2 so as to prevent the reservoir from getting over pressure. In addition, it is also important to know the properties of saline formations such as the effect of injected CO_2 to the flow of brine in the reservoir. For this purpose, there should be some tool for monitoring the reservoir behavior during the sequestration process. With the use of monitoring, it is easy to characterize the brine displaced by CO_2 and also the pressure build-up during storage process. There are different approaches for how to monitor the pressure build-up inside the saline formations such as analytical modeling and numerical simulations [4].

1.1 Aim of Thesis

This thesis aims to analyze and compare different analytical models for predicting the pressure profile in the saline formations for single injection well scenario. Then to develop analytical (or semi-analytical) models for predicting the pressure evolution for multiple well injection scenarios. Although numerical modeling is commonly used by reservoir engineers to predict the pressure distribution during CO_2 sequestration in saline formations, these numerical simulations can be very complicated during the preliminary process of reservoir evaluation as they require a large amount of data and time to produce results. Analytical model on the other hand is simplified and easy to use as it considers generic assumptions like simplified geometry, homogeneous and isotropic porous medium and do not require

spatial discretisation. They provide an abridged means for conducting preliminary test for screening of potential CO_2 storage sites. Thus, the thesis provides the new analytical approach for predicting the pressure profile for CO_2 sequestration in saline formations for multiple well scenarios. The thesis also provides examples to demonstrate how proposed multiwell injectivity analytical model can be used in reservoir for designing of CO_2 storage in saline aquifer.

The other dominant theme for various recent researches is to increase the storage capacity of potential CO_2 saline formations storage sites. The typical benchmark for the rate of CO_2 injection is only about 1 Mt/year which is very low compared to the scale necessary for the CCS to have a significant role in managing global emissions. In this study, we perform simulations for a large volume of continuous injection using multiple well injection scenario, for a period of 50 years resulting in a high total sequestration of more than 1 Gt CO_2. This thesis looks at various ways to increase the storage capacity of CO_2 in saline formations by looking at parameters like optimizing wells placement, varying injection cyclic time, flow-rate, number of wells and having relief wells to release the pressure in the reservoir by producing brine.

1.2 Organization of Thesis

This thesis mainly addresses the ways to increase the sequestration capacity of various saline aquifers for CO_2 sequestration. First, we examine various analytical models used to determine the pressure profile during CO_2 injection well in a saline aquifer. In the second part, we focus on how relative permeability affects the pressure profile and various methodologies used for estimating the saturation fronts for two-phase flow. This part includes the validation of modeling. The third part is optimization of injection and production wells to increase the injectivity of the storage site to further maximize the sequestration capacity to store large amount of CO_2 in saline formations. The thesis is organized as follows:

In chapter 1, we provide the necessary preliminaries and background. In chapter 2, we introduce various geological storage options for CO_2 sequestration. We also discuss about its leakage and trapping mechanisms. In chapter 3, we introduce various analytical models used for determining the pressure build-up for single well injection. We select a model, validate it and then apply it for multiple well scenarios. In chapter 4, we discuss optimization process to maximize the injection capacity by varying number of wells, flow-rate and placement of brine production well. Finally in chapter 5, we summarize our work and present conclusions. In addition, there are some suggestions for future work.

Chapter 2

Literature Review

2.1 Carbon Capture and Storage

It has been widely accepted fact that CO_2 emissions into the atmosphere as the major contribution to global warming. Primarily, the main cause of all this CO_2 emissions are due to the combustion of fossil fuels, emissions from cement industries, oil refineries and integrated steel mills. According to the IPCC report [1], the current concentration of CO_2 into the atmosphere is about 385ppm, which is more than 35% compared to preindustrial level. Thus, to reduce CO_2 emissions and minimization of long term climate change, various serious measures are taken. One such measure is Carbon Capture and Storage (CCS). CCS is considered to be one of the most promising technology for the reduction of CO_2 emissions into the atmosphere.

CCS is the process in which CO_2 is first separated at the emission source which is termed as Carbon Capture; then it is compressed and transported through pipelines to the storage site where it is finally injected into geological formations which is termed as Geological Carbon Sequestration. The steps involved in CCS is illustrated as below:

- **Capture of** CO_2: The pathway for capture of CO_2 originates from three main sources such as industrial processes, power plants and carbon-rich feed stocks. CO_2 capture from this sources can be performed in three processes: Post-Combustion process, Pre-Combustion process and Oxy-Combustion process. There are number of options for separating CO_2 from flue gases such as solvent scrubbing, condensation, membrane technology, absorption and adsorption.

- **Transport of CO_2**: The captured CO_2 is transported to a storage site via pipelines, tanker trucks or ships. Pipelines is considered to be cost-effective and reliable method for transportation. However, several billion tons of CO_2 has been transported via pipelines and mostly it is transported to enhanced oil recovery (EOR) fields. Ships are also considered viable option particularly when CO_2 has to be moved to overseas.

- **Storage of CO_2**: CO_2 sequestration is termed as long time storage which helps in the reduction of CO_2 emissions. The main principle behind storage is it should be safe and less environment effects. The detailed description about carbon storage are presented in Section 2.2.

2.2 Geological Carbon Storage

Once capture and transport process is carried out as described in previous Section 2.1, CO_2 should be stored for a long time so that it does not leak to the atmosphere. For a good geological storage, a reservoir should have good porosity, permeability, thickness and an impermeable cap rock which prevents the CO_2 from escaping. There are a number of geological reservoir options for storage of CO_2 such as storing CO_2 in a geological structures and oceans. The worldwide capacity for various sequestration options is illustrated in the Table 2.1.

Sequestration Options	**Worldwide Capacity (Gigatons of Carbon GtC)**
Ocean Storage	1000
Depleted Oil and Gas Reservoirs	100
Coal seams	10-100
Deep Saline Formations	100-11000
Terrestrial	10

Table 2.1: [5, 6] The worldwide capacity of potential CO_2 storage reservoirs.

Ocean storage is considered as one of the largest stores of CO_2. Injection of CO_2 in the ocean has been studied for the past three decades and it was widely considered by engineers in the late 1970s. CO_2 can be easily stored deep inside the ocean or deposited on sea floors when the supercritical CO_2 is much denser than water. It was estimated in [7] that the sink capacity for ocean storage is approximately 5000-10000 Pg C (Petagram). There are some good reasons why mineral sediments appear to offer high storage capacity. For example, cretaceous sandstone, an marine sediment was found to handle hundred

billions tons capacity for storage of CO_2 [8]. However, IPCC [1] argued that there are severe risks associated with oceanic storage such as acidification of sea water which affects the oceanic environment and marine life. Thus, the risks associated with ocean storage is predicted to be greater than geologic storage. Therefore, carbon sequestration in geological reservoirs is considered as the one of the most viable option.

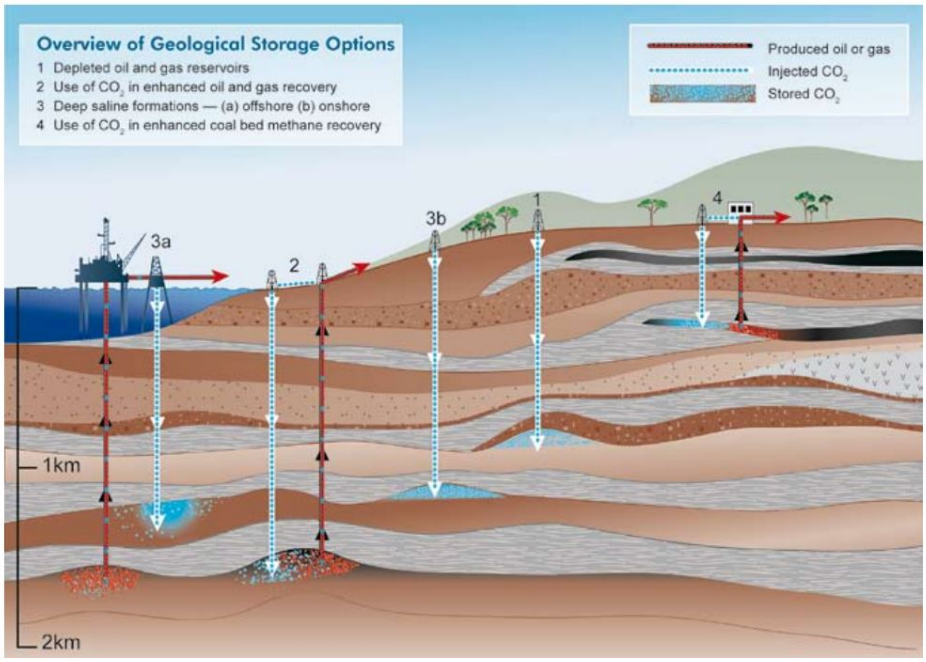

Figure 2.1: [1] An overview of geological storage options.

In 1977 Marchetti first proposed [9] geological storage of CO_2 as a mitigation option for eliminating CO_2 emissions. During the first international conference on CO_2 removal in Amsterdam (1992) [10,11], various geological storage options were explored such as storage in saline aquifers, depleted oil and gas reservoirs and combination of enhanced oil recovery (EOR) with CO_2 storage. The various geological options for CO_2 storage are illustrated in Figure 2.1. Sequestration of CO_2 inside sedimentary rocks are widely distributed around the world. For example, it was estimated in [8] that the storage capacity in geological formations were around 2020 - 14,220 Gigatons of CO_2 in USA. According to the Joule II project [12], depleted oil and gas reservoirs are considered as a viable option for storage of CO_2 because CO_2 injected acts as a solvent and it mobilizes the trapped oil to increase the oil production. During this process, CO_2 is trapped inside for million of years due to the

structural trap which prevents the sequestered CO_2 from escaping out. However, extraction of oil and gas compromises the integrity of this structural trap and causes fractures [13]. CO_2 leakage, significant pressure change and limited storage capacity knocks out depleted oil and gas reservoirs as an storage option. CO_2 storage in saline formations appears to be a viable and promising option due to high storage capacity and its availability. Therefore, this thesis focuses on modeling and optimization of injecting large volume of CO_2 in saline formations.

2.3 Carbon Sequestration in saline aquifers

Saline aquifers are sedimentary formations consisting of water permeable rock saturated with salt water, called brine. Various studies [1] have shown that saline aquifers are considered to have the highest potential to store CO_2 globally compared to other storage options such as depleted oil & gas reservoirs and coal seams. The onshore capacity for CO_2 sequestration in saline formations is often quoted as "very large" around 1000 to 11,000 Gigatons of CO_2 as seen in the Table 2.1. According to the International Energy Agency (IEA) report [14], saline aquifers can store approximately ten trillion tones of CO_2 throughout the world which is equivalent to more than ten times the total emissions estimated for next 30 years. Therefore, more attention has been given to carbon sequestration in saline aquifers.

2.3.1 Carbon Sequestration Projects Worldwide

Table 2.2 shows the list of projects which are operational and have injected CO_2 in saline formations. According to the Global CCS Institute [15], there are 22 CCS projects around the globe. The total capture capacity of these projects are around 40 million tonnes per annum. North America has the largest number of CCS projects in the world in which US has 16 CCS projects which are operational and under construction. It was approximated in [16], 15 Mt of CO_2 has been injected worldwide in saline formations at the end of 2007. Particularly, Sleiper, Snohvit and In Salah projects have injected CO_2 at a commercial scale in the order of 1 Mt of CO_2 in saline formations.

The first commercial success through the use of CO_2 sequestration was Sleipner Project which started in 1996. The Sleipner project operated by Statoil has been able to sequester about 1 Mt of CO_2 annually. This project is expected to sequester about 20 Mt of CO_2 which is equivalent to 3 percent of Norway's total annual CO_2 emissions. The In

Project	Location	Status	Capacity (kt)
Sleiper	Sleipner North Sea	Injection Underway	20000
In Salah	Krechba Algeria	Injection Underway	17000
Nagaoka	Nagaoka City Japan	Completed	10.4
Ketzin	Ketzin Germany	Injection Underway	60
Snohvit	NW of Hammerfest Barents Sea	Injection Underway	23000
Alberta Basin (Acid gas)	Alberta Canada	Injection Underway	
MGSC Decatur	Illinois USA	Planned	1000
Frio	Texas USA	Monitoring Underway	1.6
MRCSP-Cincinnati Arch	Kentucky USA	Planned	3
MRCSP-Michigan basin	Michigan USA	Monitoring Underway	10241
MRCSP-Apapalachian Basin	Ohio USA	Work Underway	3
WESTCARB Rosetta-Calpine saline	California USA	Planned	2
WESTCARB Salt river	Arizona USA	Planned	2
Gorgon	Barrow Island WA Australia	Planned	129000
SECARB Mississippi	Mississippi USA	Completed	2.75
SECARB Early	Cranfield, Mississippi USA	Injection Underway	1500

Table 2.2: [16, 17] CO_2 Sequestration projects around the world.

Salah CO_2 Storage Project is CCS project started in 2004 and has been able to store 3.8 Mt of CO_2. However, injection was suspended in 2011 due to concerns about the integrity of seal. The estimated sequestration capacity was 17 Mt of CO_2. The Snohvit Project is also an CCS project started in 2008 and CO_2 is injected into 100 meters Tubaen Formation at a depth 2600-2700 meters. This project has been able to sequester 3 Mt of CO_2 and it is expected to sequester 23 Mt of CO_2.

2.4 CO_2 subsurface Behavior and Trapping Mechanisms

During the sequestration of CO_2 in saline aquifers, injected CO_2 exists in dense phase as a supercritical fluid so as to decrease the storage volume. The critical pressure and critical temperature for CO_2 is P_c=73.82 bar and T_c=31.04^{0}C respectively. This supercritical phase is attained when injected at a depth of 800 meters or deeper. The CO_2 density ranges from 500 - 700 kg/m^3 and viscosity from 3.95×10^{-5} - 7.11×10^{-5} Pa.s depending upon the range of conditions such as pressure and temperature inside the aquifers. Supercritical CO_2 is less dense and less viscous than the resident brine under all shallow marine and continental storage conditions [18]. As CO_2 is in supercritical phase, the density of CO_2 is high which is desirable characteristics for storage. The decreased density difference between supercritical CO_2 and brine makes the geological storage more secure.

As injected CO_2 is less dense, it will rise to the top of the formation due to buoyancy forces. However, this is considered as an unfavorable condition during CO_2 sequestration in [19] because it leads to possibility of leakage of CO_2. If CO_2 escapes upwards, there is the potential for CO_2 to contaminate other geological formations and resources such as groundwater or drinking water. Thus, adequate measures are taken to evaluate the long-term storage potential in saline aquifers.

In saline aquifers, storage security is increased by various physical and chemical mechanisms mainly trapping mechanisms as seen in Figure 2.2. This mechanisms help to reduce the possibility of leakage and increase storage capacity over time. The various pathways for injected CO_2 leakage is through the pore system in low-permeability caprocks; anthropogenic pathways such as abandoned or pre-existing wells and; pore system in high-permeability caprock such as fractures or faults [1]. CO_2 leakage through abandoned wells or existing wells have the highest potential to act as a leakage conduit in CO_2 sequestration. However, there are large uncertainties about the properties of existing wells as mentioned in [20]. Thus, this pose an significant challenge for estimating leakage through wells. To reduce this leakage problem, new models need to be developed to resolve the problem of CO_2 leakage in saline formations.

Once CO_2 is injected into the subsurface, there is pressure variation near the wellbore region allowing CO_2 to enter pore spaces and causing physical and chemical mechanisms. Trapping mechanisms are discussed briefly in saline aquifers because this mechanism influences the physical state, mobility and area of extent of CO_2 plume. CO_2 sequestration in saline aquifers involves storage mechanisms [21] such as:

- Solubility trapping through dissolution in the formation water;

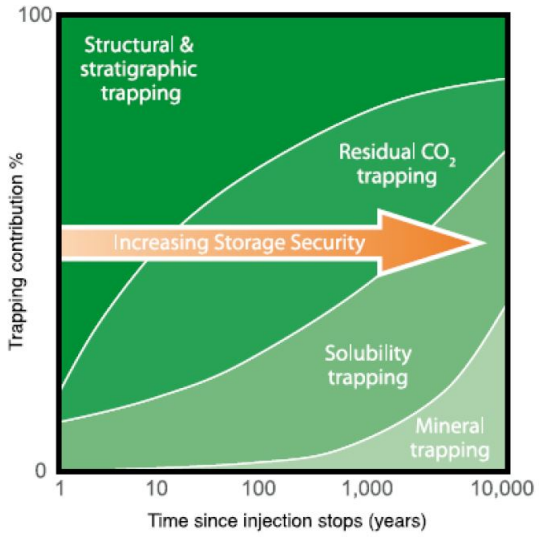

Figure 2.2: [1] Trapping contribution of the four mechanisms as a function of time.

- Hydrodynamic trapping of CO_2 plume;
- Structural and/or Stratigraphic trapping along the flow pathway;
- Mineral trapping through geochemical reactions within rocks and aquifer fluids

Thus, the capacity of CO_2 storage in saline aquifer can be considered for dissolved phase CO_2 in formation water and free-phase CO_2 in the pore space. The four main trapping mechanisms proposed to secure long term CO_2 storage are discussed below:

- **Structural and Stratigraphic Trapping**: Structural and Stratigraphic trapping mechanism is considered to be the primary mechanism during injection stage because it acts quickly and is responsible for trapping maximum amount of in situ CO_2 during early stage of injection. This mechanism uses the low permeable layer to form a barrier for CO_2 plume and the plume gets trapped due to this mechanism [22]. However, it is problematic when there is a possibility of top seal leaking through which the CO_2 could escape to the atmosphere.
- **Residual Trapping**: When the CO_2 plume is migrating, it gets trapped inside the interstitial pore space of rock formations and porous rock acting like a rigid sponge.

Over long period of time, this residually trapped CO_2 dissolves in the formation brine and helps to store CO_2 easily.

- **Solubility Trapping**: CO_2 injected into a saline aquifer, dissolves to a certain amount with brine. This mechanism takes long time and it is dependent upon temperature, pressure and salinity. When CO_2 is injected, CO_2 is considered as solute and Brine as a solvent. The solute increases brine density; as a result CO_2-brine will sink to the bottom of the rock formation, trapping CO_2 even more securely.

- **Mineral Trapping**: Mineral trapping is considered to the most secure mechanism where CO_2 reacts with soil minerals and forms a chemical compound. Once compounds are formed, in situ CO_2 can be considered to be sequestered with security. However, this mechanism will take several billion years making mineral trapping mechanism least important.

2.5 CO_2 Storage Capacity

CO_2 storage capacity is the amount of CO_2 that can be stored in the reservoir. However, estimation of storage capacity in saline formation is a complex and not a straightforward method. This is because the term "capacity" can imply two things either apparent or realistic. The apparent storage capacity is the amount of available pore space to store CO_2 in the aquifer whereas realistic storage capacity is the amount of CO_2 that can be injected into the aquifer safely which is the injection capacity of the reservoir. It is a function of number of wells, fracture pressure and their injection rates [24]. There are several factors affecting the storage capacity as cited in [23] such as pore volume of the reservoir, relative permeability, reservoir depth, salinity, heterogeneity and injection well. Although there have been many research carried out to make simple estimation of storage capacity at global scale, their attempts has been unsuccessful as shown by widely conflicting results in Figure 2.3. Bradshaw et al. [22] suggested that the best way to estimate the storage capacity is by the construction of a geological model and use of that information during reservoir modeling. There are many analytical models that look into defining the storage capacity of a potential CO_2 storage site. According to the Zhou et al. [25], injecting CO_2 causes pressurization of the reservoir which leads to expanded pore space. The injected CO_2 is trapped in these pore spaces. Other researches have proposed various criteria for long term storage of CO_2 in saline aquifers as mentioned in [11] such as :

- An aquifer should possess high porosity;

- A rock should possess high permeability in the range of 0.05-0.1μm^2 depending upon the depth;
- An aquifer depth should be located atleast at 800m so that CO_2 is in supercritical state;
- An impermeable caprock should be at the top of aquifer.

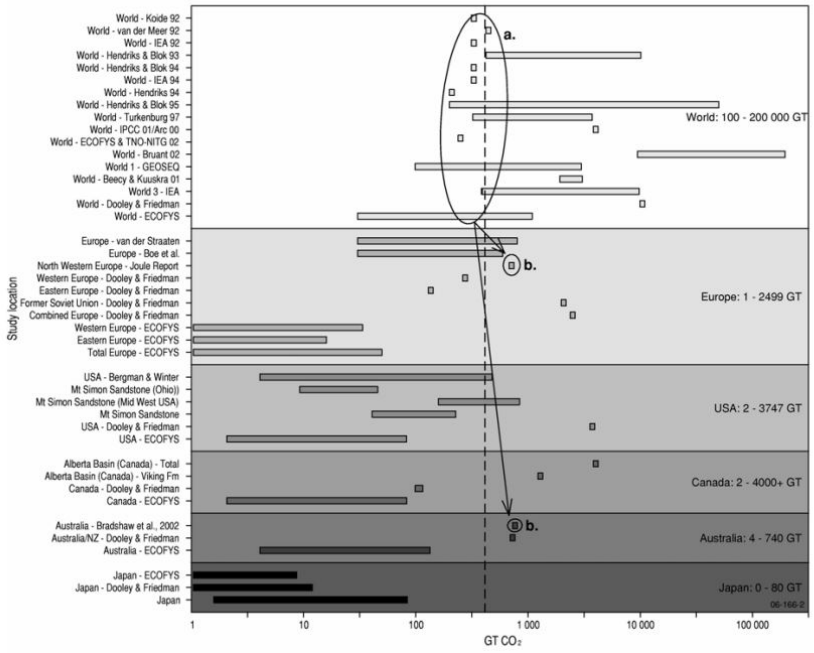

Figure 2.3: [22] Various estimates for CO_2 storage capacity around the world. Note there are world estimates (a) that are smaller than some more robust regional estimates (b).

As mentioned previously even though reservoir has volume to store it is not clear how to fill this volume, so injection capacity should be considered which is controlled by pressure build up. The amount of CO_2 that can be injected and stored into a reservoir is often pressure limited. It is important to avoid exceeding the fracture pressure in the reservoir. Formation fracture pressure is essential because the condensed gas increases the pressure within the saline formation over time and should not exceed the fracture pressure. Thus, modeling of reservoir pressure evolution is essential.

2.6 Summary

In this chapter we gave an introduction to geological carbon sequestration in Section 2.2 by going over the various storage options. We went through various carbon sequestration projects in saline formations in Section 2.3. In Section 2.4 we commented on CO_2 behavior and also discussed various trapping mechanisms in saline formations. Thus, we are interested in determining the simplified approaches for determining the pressure profile during injection process. Another area of interest is optimizing the location for injection wells and reducing the reservoir pressure with the placement of brine production well. However, there are many parameters which affect the injectivity of CO_2 and production of brine such as relative permeability, thickness, compressibility and well interference. The following chapters present many analytical models considered to calculate the pressure profile during CO_2 injection. It also focuses on single and multiple well scenarios in single phase and two-phase region accounting for all above mentioned important parameters such as permeability, solubility, well interference, leaving a window of opportunity for further development.

Chapter 3

Modeling of pressure profile for a CO_2 injection well

Modeling of CO_2 during sequestration in saline formations is an important step to predict the storage capacity of a potential CO_2 storage site. Modeling of pressure profile helps in predicting the behavior of CO_2 before and after injection in a reservoir and also pressure build-up in the saline reservoir. Thus, there should be some tool to determine the pressure build-up and CO_2 behavior inside the well. Therefore, there are various analytical and numerical models proposed to determine the pressure build-up for CO_2 injection. This models helps in assessing the injectivity and the pressure profile during injection.

In this chapter, analytical models to predict the pressure build-up for multiple well scenarios are presented for CO_2 injection in a saline formation. Solutions are first developed for single well, validated using numerical simulations and then used for multiple well scenarios. The models are applied for infinite-acting homogeneous isotropic reservoir. In addition, investigation was also conducted to study how various parameters like gas saturation and relative permeability of the reservoir affect the injectivity.

3.1 Numerical Modeling

A wide range of reservoir simulators are available around the world which are capable of simulating CO_2 injection projects. The various examples of existing numerical simulators are listed in [26] *TOUGH2*, *STOMP*, *STARS*, *ROCKFLOW*, *GEM*, *ECLIPSE*, *COORES*, *FLOTRAN*, *IPARS* − CO_2, *NUFT*, *DuMux* and *FEHM*. However, to store

large volume of CO_2, a relatively higher number of wells and optimization of placement is needed. These numerical simulators can be very time-consuming and need a lot of information.

One way of calibrating higher number of wells (multiple well cases) is to use analytical modeling to a more simplified physical problem. Therefore, there is research carried out to develop analytical and semi-analytical model for CO_2 injection in saline formations which is discussed briefly in Section 3.2. We used CMG′s commercial black oil simulator, *IMEX* for just validating our analytical model.

3.2 Analytical Modeling

Analytical models have been widely used by reservoir engineers as a fast and efficient means for determining the pressure build-up inside the reservoir beforehand. These analytical models are viable and easy tool in determining well operations like gas injection, brine production, well simulation and gas hydrate production [27]. Analytical models are also used for well test analysis in the reservoir engineering. From [28], it can be seen that well test analysis helps to determine the average reservoir pressure, verifying skin effect, permeability and also for identifying the fluid behavior inside the reservoir. Analytical models are based on simple assumptions like simple geometry of flow, homogeneous and isotropic reservoir which do not require spatial discretisation. Recently, Nordbotten et al. [29, 30] argued that analytical models are simple, easy methods to provide estimates of environmental and hydrologic consequences for CO_2 injection. Person et al. [31] suggested that the analytical models help to capture the relevant physics behind CO_2 injection without relying on numerical modeling. Thus, there are various analytical models proposed and adjusted to determine the pressure build-up during CO_2 injection in saline formations. The description of various analytical model are discussed in the next Section 3.3.

3.3 Modeling CO_2 injection (Two Phase flow)

3.3.1 Single Well Scenarios

Quite recently, various analytical and semi-analytical models for single well injection have been developed for CO_2 injection as multi-phase flow in saline formations. When CO_2 is injected in a saline aquifer, CO_2 flows as a single phase flow surrounded by a two

phase region where the saturation varies from 100% CO_2 to 100% brine. All these models assume Buckley-Leverett displacement theory (BL) [32]. BL displacement method [33] describes two phase flow as one dimensional immiscible flow.

Nordbotten et al. [34] built an analytical solution to describe the space-time evolution of CO_2 plume. The model extends the underlying philosophy of one dimensional radial form of the BL theory. In this model, the residual saturation of CO_2 is set to unity and phase viscosities are kept constant. The phase saturation and fluid viscosities are assumed constant. This model helps in estimating the spread of CO_2 plume which gives us an idea of extent of CO_2 plume, thereby avoiding any chances of possible leakages. The model predicts a quick estimate of the CO_2 plume during the lifetime of operation. The pressure build-up for two-phase region at the injection well is given by

$$P(r_{well}, t) = Pi - \frac{q}{2\pi\lambda_w k} \int_r^R \frac{1}{\mathrm{r}((\lambda - 1)\mathrm{b}(\mathrm{r}) + \mathrm{B})} \, \mathrm{d}r, \tag{3.1}$$

where λ_w is brine mobility, b denotes the thickness of CO_2 plume and B denotes the thickness of the formation.

Zhou et al. [25] developed a similar analytical model for CO_2 sequestration in closed and semi-closed saline formations in open systems. The model helps in predicting the pressure build-up and also its storage efficiency factor during CO_2 injection. The underlying assumption for this analysis is that pressure build-up is uniform and it is independent of formation permeability. This model is not considered, as on doing initial sensitivity analysis we found that the reservoir pressure build-up is very sensitive to formation permeability. Recently, Burton et al. [35] developed a simple one dimensional analytical model for CO_2 injection in terms of phase mobility and the speed of the saturation fronts. This model was derived by using Darcy law and modified form of BL fractional flow theory. They followed the modified form of BL fractional flow theory to determine the position of saturation fronts in two phase region. The speed of saturation fronts defines three regions of flow: dry CO_2 in the near-wellbore region, BL or two phase region and Brine region far from the well. The model ignored the effect of compressibility. The model estimates the phase mobilities in each region from the relative permeability curve. The total pressure drop across the reservoir is given by

$$Pw = Pi + \frac{q}{2\pi kh} \left[\frac{\mu_g}{k_{rg}} \ln\left(\frac{r_{dry}}{r_w}\right) + \left(\frac{k_{rg}}{\mu_g} + \frac{k_{rw}}{\mu_w}\right)^{-1}|_{S_g = S_{avg}} \ln\left(\frac{r_{BL}}{r_{dry}}\right) + \mu_w \ln\left(\frac{r_e}{r_{BL}}\right) \right], \tag{3.2}$$

where r_{BL}, r_{dry} denotes the radial front in BL and CO_2 region respectively. In order to move ahead with this model we need to calculate the value of the radial fronts r_{BL} and r_{dry} which is difficult to estimate.

Mathias et al. [32] developed an analytical and semi-analytical model to determine pressure build-up for CO_2 injection which is a similar approach proposed by Nordbotten et al. [34]. This model develops approximate solutions for pressure build-up inside the reservoir on CO_2 injection using the method of matched asymptotic expansions including the effect of compressibility. Recently, Mathias et al. [36] also developed an analytical model to determine the approximate solutions for pressure build-up of finite radial extent. They developed analytical model in saline formations using the large-time approximation method for estimation of maximum pressure build-up. Mathias et al. [37] showed that the pressure build-up at the injection well can be approximated by

$$Pw = P_0\Big[-\frac{1}{2}\ln\Big(\frac{t_0}{2\gamma t}\Big) - 1 + \frac{1}{\gamma} - \frac{1}{2\gamma}[\ln\Big(\frac{\alpha}{2\gamma^2}\Big) + 0.5772] + \beta)\Big], \tag{3.3}$$

where β denotes dimensionless Forchheimer parameter, γ denotes viscosity ratio and α denotes dimensionless compressibility. However, this model is very complex and requires a lot of dimensionless parameter estimation.

Ehlig-Economides and Economides [38] further extended the analytical model developed by Burton et al. [35] based on the modified BL fractional flow theory. This model follows BL theory to predict the relative permeability values in the two phase region at the average CO_2 saturation. This model accounts for closed boundary reservoir formation by applying factor 0.472 in the last natural logarithm term in Equation 3.4. It also takes into account the effect of volume on the reservoir and compressibility effect to attain CO_2 injection. The total pressure distribution is given by

$$Pw = Pi + \frac{q}{2\pi kh}\left[\frac{\mu_g}{k_{rg}}\ln\Big(\frac{r_{dry}}{r_w}\Big) + \Big(\frac{k_{rg}}{\mu_g} + \frac{k_{rw}}{\mu_w}\Big)^{-1}|_{S_g=S_{avg}}\ln\Big(\frac{r_{BL}}{r_{dry}}\Big) + \mu_w\ln\Big(\frac{0.472r_e}{r_{BL}}\Big) + \frac{V_{CO_2}}{V_r c_t}\right], \tag{3.4}$$

where V_{CO_2} denotes the total volume of CO_2 to be injected, V_r is the minimum required pore volume to store the volume of CO_2 and c_t is total compressibility including rock, brine and CO_2 compressibility. This approach is valid for a closed, with no-flow boundaries. This simplification is inappropriate for regional CO_2 storage modeling, as it is well understood

that the shales that typically surround storage reservoirs have non-zero permeabilities. In addition, this model is complex as we need to predict the velocity and radial fronts.

Azizi and Cinar [39] developed an analytical model to determine the pressure build-up for CO_2 injection well in a saline aquifer for three types of formations such as infinite acting, closed boundary and constant boundary formation. The underlying assumptions include a horizontal, homogeneous aquifer with constant fluid properties. This model takes into account the effects of relative permeability and CO_2 dissolution in brine. They have applied dimensionless technique to solve for the fluid pressures in the three regions of an infinite-acting saline formation as shown below (Equation 3.5, 3.6 and 3.7):

$$\frac{1}{r_D}\frac{\partial}{\partial r_D}\left(r_D\frac{\partial P_{D1}}{\partial r_D}\right) = \frac{\partial P_{D1}}{\partial t_D}, \qquad 0 < r_D < r_{Ddry}. \tag{3.5}$$

$$\frac{1}{r_D}\frac{\partial}{\partial r_D}\left(r_D\frac{\partial P_{D2}}{\partial r_D}\right) = \frac{1}{F_{\lambda g}\eta_{D2}}\frac{\partial P_{D2}}{\partial t_D}, \qquad r_{Ddry} < r_D < r_{DBL}. \tag{3.6}$$

$$\frac{1}{r_D}\frac{\partial}{\partial r_D}\left(r_D\frac{\partial P_{D3}}{\partial r_D}\right) = \frac{1}{\eta_{D3}}\frac{\partial P_{D3}}{\partial t_D}, \qquad r_{DBL} < r_D < \infty. \tag{3.7}$$

The initial and boundary conditions for the above Equations (3.5, 3.6 and 3.7) are as follows:

$$P_{D1} = P_{D2} = P_{D3} = 0, \quad t_D = 0. \tag{3.8}$$

$$r_D\frac{\partial P_{D1}}{\partial r_D} = -1, \quad r_D \to 0. \tag{3.9}$$

$$P_{D1} = P_{D2}, \quad r_D = r_{Ddry}. \tag{3.10}$$

$$\frac{\partial P_{D1}}{\partial r_D} = F_{\lambda g}\frac{\partial P_{D2}}{\partial r_D}, \quad r_D = r_{Ddry}. \tag{3.11}$$

$$P_{D2} = P_{D3}, \quad r_D = r_{DBL}. \tag{3.12}$$

$$\frac{\partial P_{D3}}{\partial r_D} = F_{\lambda w} \frac{\partial P_{D2}}{\partial r_D}, \quad r_D = r_{DBL}. \tag{3.13}$$

$$P_{D3} = 0, \quad r_D \to \infty. \tag{3.14}$$

The equations have dimensionless parameters such as P_D, t_D, r_D and ϵ which are the dimensionless pressure, time, radial distance and injection rate from injector respectively.

$$P_D = \frac{2\pi hkk_{rg}(P - P_i)}{qB_g\mu_g}, \quad t_D = \frac{kk_{rg}t}{\mu_g\phi r_w^2 c_{tg}},$$

$$r_D = \frac{r}{r_w}, \qquad \epsilon = \frac{qc_{tg}\mu_g B_g}{4\pi hkk_{rg}}.$$

We need to calculate the model parameters such as η_{D2}, η_{D3} and $F_{\lambda g}$ which are diffusivity ratios and dimensionless total mobility as defined below:

$$\eta_{D2} = \frac{c_{tg}}{c_t} \mid_{S_{avg}} \tag{3.15}$$

$$\eta_{D3} = \frac{c_{tg}}{c_{tw}} \frac{\lambda_w}{\lambda_g} \tag{3.16}$$

$$F_{\lambda g} = \frac{\lambda_g + \lambda_w}{\lambda_g} |_{S_{avg}} \tag{3.17}$$

Now, on applying Laplace transform on Equations 3.5, 3.6 and 3.7 using initial conditions yields:

$$\frac{\partial^2 P_{D1}}{\partial^2 r_D} + \frac{1}{r_D}\frac{\partial P_{D1}}{\partial r_D} - sP_{D1} = 0. \tag{3.18}$$

$$\frac{\partial^2 P_{D2}}{\partial^2 r_D} + \frac{1}{r_D}\frac{\partial P_{D2}}{\partial r_D} - \frac{s}{F_{\lambda g}\eta_{D2}}P_{D2} = 0. \tag{3.19}$$

$$\frac{\partial^2 P_{D3}}{\partial^2 r_D} + \frac{1}{r_D}\frac{\partial P_{D3}}{\partial r_D} - \frac{s}{\eta_{D3}}P_{D3} = 0. \tag{3.20}$$

where s is the Laplace-transform variable.

The solutions of Equations 3.18, 3.19 and 3.20 can be written as:

$$P_{D1} = B[A + K_0(r_D\sqrt{s})]. \tag{3.21}$$

$$P_{D2} = B\Big[C + DK_0\Big(r_D\sqrt{\frac{s}{F_{\lambda g}\eta_{D2}}}\Big)\Big]. \tag{3.22}$$

$$P_{D3} = B\Big[EI_0\Big(r_D\sqrt{\frac{s}{\eta_{D3}}}\Big) + FK_0\Big(r_D\sqrt{\frac{s}{\eta_{D3}}}\Big)\Big]. \tag{3.23}$$

where I_0 and K_0 are Bessel functions. Using initial conditions (Equations 3.9 and 3.14), we get $B = \frac{1}{s}$ and $E = 0$. Now, using the inverse Laplace transformation and applying boundary conditions to Equations 3.21, 3.22 and 3.23 yields:

$$P_{D1} = A - \frac{1}{2}E_i\Big(-\frac{r_D^2}{4t_D}\Big), \qquad t_D \geq \frac{r_D^2}{4\xi_{Ddry}}. \tag{3.24}$$

$$P_{D2} = C - \frac{D}{2}E_i\Big(-\frac{r_D^2}{4F_{\lambda g}\eta_{D2}t_D}\Big), \qquad \frac{r_D^2}{4\xi_{DBL}} \leq t_D \leq \frac{r_D^2}{4\xi_{Ddry}}. \tag{3.25}$$

$$P_{D3} = -\frac{F}{2}E_i\Big(-\frac{r_D^2}{4\eta_{D3}t_D}\Big), \qquad t_D \leq \frac{r_D^2}{4\xi_{DBL}}. \tag{3.26}$$

where ξ_{Ddry} and ξ_{DBL} are functions of ϵ and for lower values of ξ_{Ddry} and ξ_{DBL}, the value of the coefficients are estimated as follows:

$$F = \frac{\lambda_g}{\lambda_w}, \qquad D = \frac{1}{F_{\lambda g}},$$

$$A = \frac{1}{2}E_i(-\xi_{Ddry}) - \frac{1}{2F_{\lambda g}}E_i\Big(-\frac{\xi_{Ddry}}{F_{\lambda_g}\eta_{D2}}\Big) + \frac{1}{2F_{\lambda g}}E_i\Big(-\frac{\xi_{DBL}}{F_{\lambda g}\eta_{D2}}\Big) - \frac{1\lambda_g}{2\lambda_w}E_i\Big(-\frac{\xi_{DBL}}{\eta_{D3}}\Big),$$

$$c = \frac{1}{2F_{\lambda g}}E_i\Big(-\frac{\xi_{DBL}}{F_{\lambda g}\eta_{D2}}\Big) - \frac{1\lambda_g}{2\lambda_w}E_i\Big(-\frac{\xi_{DBL}}{\eta_{D3}}\Big). \tag{3.27}$$

On substituting the values of these coefficients, we get the final solution for predicting the pressure build-up in three regions are as follows:

$$P_D = -\frac{1}{2}E_i\Big(-\frac{r_D^2}{4t_D}\Big) + \frac{1}{2}E_i(-\xi_{Ddry}) - \frac{1}{2F_{\lambda g}}E_i\Big(-\frac{\xi_{Ddry}}{F_{\lambda_g}\eta_{D2}}\Big) + \frac{1}{2F_{\lambda g}}E_i\Big(-\frac{\xi_{DBL}}{F_{\lambda g}\eta_{D2}}\Big) - \frac{1\bar{\lambda}_g}{2\bar{\lambda}_w}E_i\Big(-\frac{\xi_{DBL}}{\eta_{D3}}\Big) \tag{3.28}$$

where $t_D \geq \frac{r_D^2}{4\xi_{Ddry}}$.

$$P_D = -\frac{1}{2F_{\lambda g}}E_i\Big(-\frac{r_D^2}{4F_{\lambda g}\eta_{D2}t_D}\Big) + \frac{1}{2F_{\lambda g}}E_i\Big(-\frac{\xi_{DBL}}{F_{\lambda g}\eta_{D2}}\Big) - \frac{1\bar{\lambda}_g}{2\bar{\lambda}_w}E_i\Big(-\frac{\xi_{DBL}}{\eta_{D3}}\Big), \tag{3.29}$$

where $\frac{r_D^2}{4\xi_{DBL}} \leq t_D \leq \frac{r_D^2}{4\xi_{Ddry}}$.

$$P_D = -\frac{1\bar{\lambda}_g}{2\bar{\lambda}_w}E_i\Big(-\frac{r_D^2}{4\eta_{D3}t_D}\Big), \tag{3.30}$$

where $t_D \leq \frac{r_D^2}{4\xi_{DBL}}$.

The final total pressure build-up is given by equation below:

$$Pw = Pi + \left(\frac{P_D q B_g \mu_g}{2\pi h k k_{rg}}\right), \tag{3.31}$$

where ξ_{DBL} and ξ_{dry} denotes the movement of the fronts in BL and dry regions respectively; η_{D2} and η_{D3} denotes dimensionless diffusivity ratio and $F_{\lambda g}$ represents the total mobility.

In our modeling, we use the analytical model for single well proposed by [39] which takes into account the effects of relative permeability and CO_2 dissolution in brine. This model is a simplified assumption as we don't need to find the accurate values for the velocity fronts and the radial fronts r_{BL} and r_{dry} respectively. Instead we used the modified fluid pressure build-up equation shown for three regions in terms of injection time which is more practical approach. This model help us to estimate the pressure build-up developed due to CO_2 injection. The detailed description of the approximation and diffusivity equations are given in [39]. Also, recent work by Joshi [40] has demonstrated the use of Azizi and Cinar [39] approach for assessing the storage capacity for the Nisku aquifer. The model was also applied for the geological setting with multi-wells further validating the model applicability to be considered for multiple injection well case scenarios. We extended the work done by looking into the sensitivity of saturation fronts on predicting the various parameters during modeling, as Joshi's [40] work considers only one approach for determining the saturation fronts. We also implemented the analytical model on various other reservoirs by identifying the fitting parameter for predicting the saturation fronts and model parameters which can be used to determine the pressure build-up during CO_2 injection in saline formations for each case.

There are several underlying assumptions such as the reservoir is homogeneous, infinite acting, isothermal and isotropic. A fully penetrating vertical well is used for injection of CO_2 in saline formation at a constant injection rate. Reservoir compressibility, thickness, permeability are all kept constant. The effect of capillary, gravity and skin factor are neglected for simplicity. On injecting CO_2 into the saline aquifer, there is a creation of three regions in the formation as shown in Figure 3.1.

Region *1* shows a dry gas region where CO_2 is dissolved in brine phase. Region *2* represents two phase flow where brine is saturated with CO_2 or CO_2 is saturated with brine. Region *3* shows the fully saturated brine phase. The radial boundaries for the three regions *i.e.* single phase CO_2, two phase region or BL and single phase brine are r_{dry}, r_{BL} and r_e respectively. As a result, we have two saturation fronts dry (S_{gDry}) and BL saturations (S_{gBL}) between these three regions. The saturation distribution in these regions do not

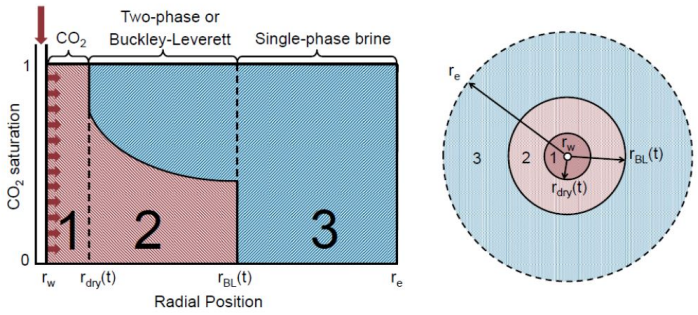

Figure 3.1: [35] Schematic representation of three phase regions around CO_2 injection well.

consider gravity segregation into account as we neglect gravity forces. With the saturation profile, the analytical model for predicting the pressure profile can be determined.

3.4 Determination of Saturation Profile

Flow in two phase flow are of fundamental importance to many problems related to the storage of CO_2. Wu et al. [41] concluded that the multi-phase flow when compared to single phase flow are very complicated and not clear due to complex interaction of different fluid phase. Thus, the fundamental understanding of flow in multi-phase flow is solved by BL displacement study on fractional flow theory [33]. The BL displacement theory helps to determine the saturation profile with a sharp front along the flow direction by ignoring the gravity and capillary effects. Thus, the saturation profile can be determined by the various approaches as mentioned in by Noh et al. [42], Welge [43] and Woods et al. [44].

Relative permeability and fractional flow curves need to be defined to build the saturation fronts. First, the relative permeability curve is plotted to determine the fractional flow curve. In our study we modeled the reported data (for different cases) and fitted it using the relative permeability formulation by Corey approach [45].

$$k_{rg} = k^0_{rg}\left[\frac{S_g}{1-S_{wr}}\right]^m, \qquad k_{rw} = \left[1-\frac{S_g}{1-S_{wr}}\right]^n, \tag{3.32}$$

where g and w represent CO_2 and Brine phases respectively, S_g is the gas saturation, S_{wr} is the residual brine saturation, k^0_{rg} is gas endpoint relative permeability, m and n are corey gas and brine components respectively.

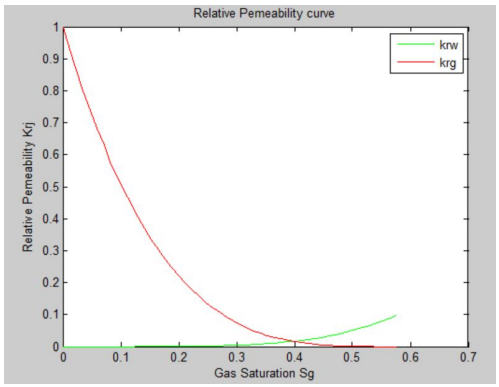

(a) Relative Permeability Curve.

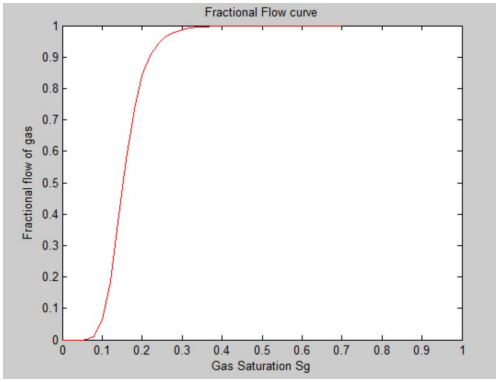

(b) Fractional Flow Curve.

Figure 3.2: Relative Permeability and Fractional Flow for Viking aquifer.

With the help of Equation 3.32, the relative permeability can be plotted with respect to gas saturation S_g as shown in Figure 3.2.

Now, we can evaluate the fractional flow curve for the determination of two saturation fronts from the relative permeability curve. Fractional flow is dependent only on relative permeabilities and viscosities of fluids. Fractional flow equation is defined as the model used for the determination of fraction of total fluid flow for a certain period of time. Once the saturation profile is known, the diffusivity pressure Equation 3.31 for two phase flow are solved. There are several methods to evaluate the saturation fronts in two phase flow. All these models have underlying assumptions such as one dimensional homogeneous system, porous medium, two phase flow, no gravity and capillary forces.

In the first approach proposed by [42], the saturation fronts is determined using the fractional flow theory. Figure 3.3 shows the schematic representation of fractional flow curve of a gaseous phase where CO_2 displaces brine in a saline aquifer.

The fractional flow for two phase can be evaluated as:

$$f_{Brine} = \frac{1}{1 + \left(\frac{k_{rw}}{k_{rg}}\right)\left(\frac{\mu_g}{\mu_w}\right)}, \qquad f_{CO_2} = \frac{1}{1 + \left(\frac{k_{rg}}{k_{rw}}\right)\left(\frac{\mu_w}{\mu_g}\right)}, \tag{3.33}$$

where k_{rg} is CO_2 relative permeability, k_{rw} is Brine relative permeability, μ_g is CO_2 viscosity and μ_w is Brine viscosity.

Using Equation 3.33, the fractional flow curve is plotted (refer to Figure 3.2). Now, to determine the saturation fronts *i.e.* Dry front saturation S_{gDry} and BL front saturation

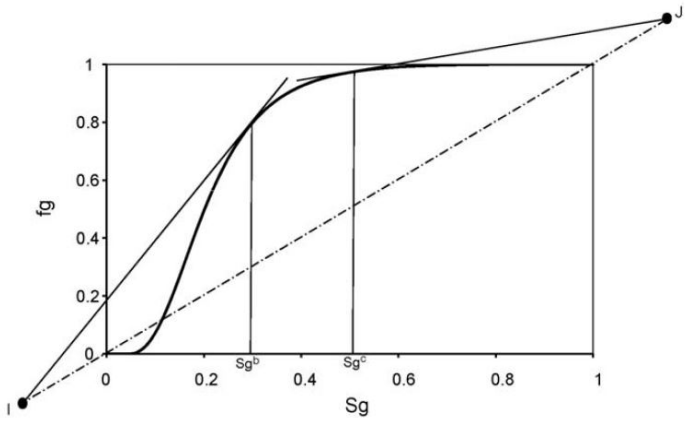

Figure 3.3: [42] Fractional flow curve by Noh et al. approach

S_{gBL}, we draw tangents on fractional flow curve from two points (*i.e.* points I and J) located on the slope line drawn from origin (refer to Figure 3.3). Point I and Point J represents the initial and injection conditions respectively. A tangent line drawn from point I to gaseous phase are evaluated at equilibrium between the gaseous (CO_2) and aqueous (*brine*) phase. The slope of the line from point I represents the specific velocity of fast shock *i.e.* v_{BL}. The second tangent drawn from point J to the fractional flow curve exists where the dry gaseous phase (CO_2) evaporates the aqueous phase (*brine*). The slope of this line is referred to as specific velocity of slow shock v_{dry}. According to this approach, the two points are referred as retardation factors such as D_{BL} and D_{Dry} for brine displacing CO_2 and CO_2 displacing brine respectively.

The placement of the shocks (points I and J) are obtained by [46] using graphical approach. In this approach, the retardation factors D_{BL} (S_g^I, f_g^I) and D_{Dry} (S_g^J, f_g^J) are defined as:

$$I = (S_g^I, f_g^I) = \left(\frac{\rho_a \omega_{CO_2,a}}{\rho_a \omega_{CO_2,a} - \rho_g \omega_{CO_2,g}}, \frac{\rho_a \omega_{CO_2,a}}{\rho_a \omega_{CO_2,a} - \rho_g \omega_{CO_2,g}}\right). \tag{3.34}$$

$$J = (S_g^J, f_g^J) = \left(\frac{\rho_a \omega_{Brine,a}}{\rho_a \omega_{Brine,a} - \rho_g \omega_{Brine,g}}, \frac{\rho_a \omega_{Brine,a}}{\rho_a \omega_{Brine,a} - \rho_g \omega_{Brine,g}}\right). \tag{3.35}$$

Once the retardation factors (I *and* J coordinates) are evaluated using Equations 3.34 and 3.35, we move ahead and determine the two saturation fronts S_g^b and S_g^c as seen

in Figure 3.3. These saturation fronts help us predict the analytical model for determining the pressure profile.

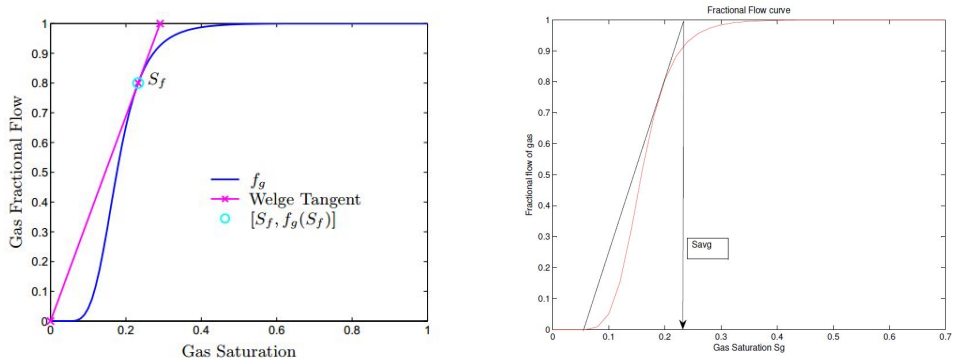

(a) Determination of front shock S_f.

(b) Determination of average saturation front S_{avg}.

Figure 3.4: [43] Fractional flow curve by Welge.

We used another graphical approach proposed by Welge [43]. In this approach, the fractional flow is plotted with the help of relative permeability data. As shown in Figure 3.4, the tangent drawn originates at the initial gas saturation. The tangent point represents the gas saturation at the displacement front. The slope of this tangent line represents the speed of the saturation fronts *i.e.* S_{gBL} and S_{dry}. As shown in the Figure 3.4, the average saturation front (*i.e.* S_{avg}) are estimated using the Welge tangent method. This approach can be used for the determination of average saturation front when the initial saturation is uniform.

Our another approach for the evaluation of saturation fronts is determined by using Woods et al. [44]. In this method, the saturation fronts are obtained by drawing tangents on fractional flow curve from origin (refer Figure 3.5). In this case, the fractional flow is defined as seen in Equation 3.36. Thus, two saturation fronts i.e. S_{gBL} and S_{gDry} are evaluated by this approach.

$$f_g = \frac{f_{g-0}}{S_{g-0}}. \tag{3.36}$$

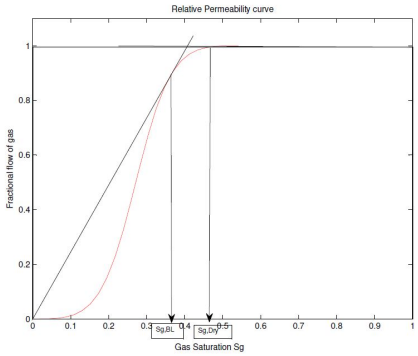

Figure 3.5: [44] Fractional flow curve by Woods et al.

3.5 Pressure profile for Single Well scenarios

After the prediction of saturation fronts, the rise in reservoir pressure due to injection of CO_2 can easily be determined. The primary objective during injection process is continuous measurement of reservoir pressure versus time and the maintenance of pressure below the fracture pressure. According to [47], the formation pressure is used in predicting the volumetric calculation, dynamic reservoir property determinations such as relative permeability, reservoir characterization and fluid characterization such as determination of phase behavior and fluid properties.

For the study to predict reservoir pressure with respect to time, we have used the analytical model by [39] for two phase model. Equations 3.31, 3.28, 3.29 and 3.30 are used for determining pressure build-up for single CO_2 injection in saline formations. The input parameters used to calculate the pressure build-up are listed as seen in the Table 3.1. We used the properties of the reservoir similar to those used in Berkeley Laboratory study [48].

We evaluated two saturation fronts using all the different approaches to compare our results (refer Table 3.2). Table shows how the maximum BHP profile changes with different value of average saturation fronts (S_{avg}) emphasizing the importance of validating the model before using it to perform further analysis. As the first step, we use the relative permeability reported in Berkeley data [48] to derive the fractional flow curve for our case. To model the fractional flow curve we used reservoir parameters like μ_g=0.062cP, μ_w=0.84cP, S_{wr}=0.332 and S_{gr}=0.05. Using all this parameters, we obtain the fractional flow (f_g) curve shown in Figure 3.6(a). There are many approaches to predict the saturation fronts.

The most commonly used method in the literature is Noh et al. approach. Using

Parameters	**Value**
Porosity (ϕ)	0.12
Permeability (k)	100 mD
Thickness (h)	100 m
Brine Viscosity (μ_w)	0.84 cP
CO_2 Viscosity (μ_g)	0.062 cP
Rock Compressibility (c_r)	1.45×10^{-10} 1/Pa
Brine Compressibility (c_w)	1×10^{-9} 1/Pa
Gas Formation Volume Factor (B_g)	0.0022 rB/SCF
Injection Rate (Q)	81.02 m^3/s
Time (t)	50 years
Radius of well (r_w)	0.076 m
Initial Pressure (P_i)	1.2×10^7 Pa
Fracture Pressure (P_f)	2.7×10^7 Pa
Relative Permeability Data	
Brine residual saturation (S_{wr})	0.332
CO_2 residual saturation (S_{gr})	0
Brine relative permeability component (n)	3
CO_2 relative permeability component (m)	3
CO_2 endpoint relative permeability (k_{rg0})	0.0
Brine endpoint relative permeability (k_{rw0})	1

Table 3.1: Parameters for Single well modeling using Berkeley Laboratory study [48].

Approach	S_{gBL}	S_{gdry}	S_{avg}	**Maximum BHP**
Noh et al.[42]	0.22	0.31	0.26	24.5 MPa
Woods et al.[44]	0.22	0.35	0.29	23 MPa
Welge [43]			0.19	26.5 MPa
CMG Numerical Model				28 MPa
Analytical Model			0.185	27.5 MPa

Table 3.2: Determination of average saturation fronts by various graphical approach.

this approach, we calculated the coordinates of points I and J which are (-0.05, -0.05) and (1.0469, 1.0469) respectively. The average saturation front for Berkeley parameters was obtained to be 0.26 resulting to a reservoir pressure of 24.5MPa which is very less compared to numerical model $i.e.$ 28MPa (refer to Figure 3.6).

The next approach to get a closer approximation to the actual reservoir pressure was by using Welge tangent method. In this approach, we draw tangent from initial gas saturation ($i.e.$ in our case S_g=0) to the fractional flow curve (refer Figure 3.6) to give us

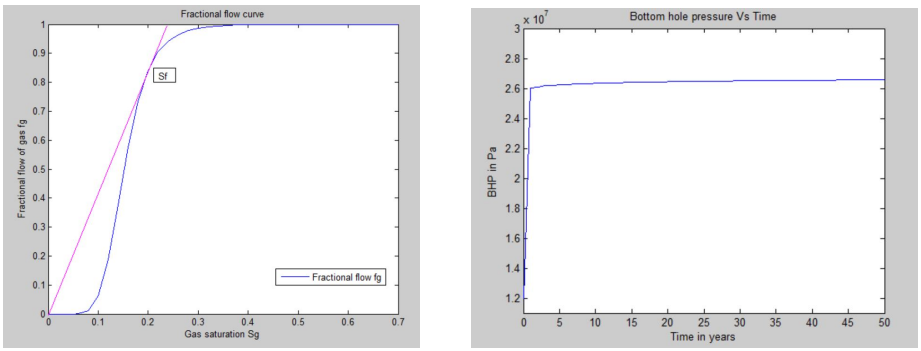

(a) Fractional flow curve. (b) Pressure build-up profile.

Figure 3.6: Fractional flow and pressure profile for Berkeley study.

the point (0.19, 0.75). Using this technique, we get the average saturation fronts (S_{avg}) as 0.19 resulting to a reservoir pressure of 26.5MPa which is closer to the one obtained from the numerical model($i.e.$ 28MPa).

As we know the saturation front is very sensitive to the reservoir pressure so in order to get a better estimation of the saturation front, we extended the Welge tangent approach further by doing iterations. In this case, we followed the same procedure of plotting the relative permeability curve using the gas saturation (S_g), gas relative permeability (k_{rg}) and brine relative permeability (k_{rw}) using the Berkeley parameters listed in [48]. Once the relative permeability data is plotted, we plotted the fractional flow curve. In order to get the best fitting parameter, we find the slope on the fractional flow curve between the points 0.18 and 0.20 originating from initial gas saturation (S_g), as we found the value of S_{avg} from Welge approach to be 0.19. On doing so, we get the value of average saturation front (S_{avg}) to be 0.185. The pressure build-up was found to be 27.5MPa which is in closer agreement with the numerical model ($i.e.$ 28MPa). Thus, we proceeded with the modified welge method for the determination of saturation fronts.

Once the accurate saturation fronts are determined, all the analytical model parameters can be determined and the analytical two phase model can be run. The analytical model for single well scenarios are compared with numerical modeling for validation purpose. The $CMGs$ commercial simulator is used for validating our model. Figure 3.7 shows reservoir pressure for single well CO_2 injection in saline formations. The BHP is constrained to less than 90% of fracture pressure over the entire injection period so as to maintain the integrity of the reservoir and prevent any leakage. In our case, BHP reaches 2.7×10^7Pa which is similar to the result obtained by the numerical simulator ($i.e.$

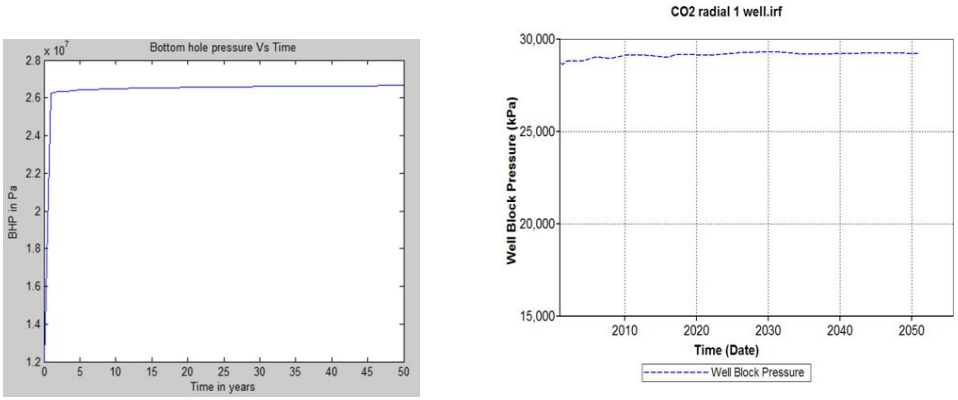

(a) Analytical Modeling. (b) Numerical Modeling.

Figure 3.7: Comparison of Analytical model with Numerical simulations.

28,000kPa) implying that our analytical model is valid.

As shown in the Figure 3.7, the analytical modeling and numerical solution for a single well CO_2 injection in saline formations are in close agreement.

3.6 Multiple Well Scenarios

As mentioned in the Section 3.3.1 for single well scenarios, there are various analytical models proposed for single well to determine reservoir pressure for CO_2 injection in a saline formations. However, in order to inject maximum amount of CO_2 at a commercial rate, more than one well is required to maximize the injectivity of CO_2. Thus, modeling for multiple well cases should be considered in order to achieve high injection capacity.

Determination of injection capacity for multiple well cases is not straightforward process but can be developed by extending the model from a single well scenario. This is because increase in pressure caused by one well can easily affect the injection rate for another well if both the wells are placed in same formation. However, there is no analytical model developed in the literature focusing on multiple well and multiphase system focusing on CO_2 injectivity in saline formations. When CO_2 is injected in saline aquifer, two phase flow of CO_2 and brine exists. But, modeling for two phase scenario is complicated as it is dependent upon a number of factors such as relative permeability, formation fracture pressure, reservoir permeability, capillary pressure, dissolution effects of CO_2, injection well

location relative to the boundary of aquifer and structural gradient changes at reservoir level [49,50]. The later part of the Section deals with the development of analytical model considering two phase flow to determine the pressure profile for multiple well scenarios.

3.6.1 Modeling for Multiple Well scenarios

There are various studies on multiple well scenarios in petroleum literature. In 1999, Marhaendrajana et al. [51] developed multiwell solution for the pressure behavior of a well in a bounded reservoir using the superposition principle. The model was assumed to be homogeneous bounded rectangular reservoir with constant thickness, full penetrating wells and location of wells were arbitrary. They used the combined approach of single phase gas pseudopressure with a homogeneous reservoir model for determination of pressure profile. Li and Yang [52] extended the multiwell model developed by [51]. In this model, they considered well interference effects for both injection and production wells. However, all these analytical models are developed for oil and gas injectivity.

The literature review on multiple well scenarios for CO_2 injection in a geological formation are sparse. In 2008, Zakrisson et al. [53] used single phase steady state flow to assess the effects of well interference during CO_2 injection in subsurface formations. They used the superposition technique to develop multiwell injectivity model. They presented the results of effect of number of wells, formation permeability, well spacing and total injection rate on well interference. In 2009, Ghaderi et al. [54] presented the investigation of injection of CO_2 in a saline aquifer. They used numerical simulations to determine the minimum number of wells required to store desired amount of CO_2 in an infinite acting reservoir. They also presented sensitivity analysis of reservoir parameters and their effect on storage of CO_2. In 2011, Pooladi-Darvish et al. [55] developed an analytical solution for multiple wells injectivity for CO_2 injection in saline aquifer as a function of number of wells and distance between wells. They used single phase steady state flow and developed multiwell model using superposition technique. The model assumed to be homogeneous reservoir with constant thickness.

However, all these models assume single state phase flow model for simplicity. A single phase model approach does not require knowledge of relative permeability data and it is more practical and convenient during analysis of well data. A two phase model approach is very complicated and requires knowledge of relative permeability data set as well as a pressure saturation function for the determination of pressure profile and mobility [51]. There are no analytical models in the CO_2 sequestration literature focusing on modeling of multiple well and multi-phase flow system for CO_2 storage in saline formations. Thus,

the following Section presents the new analytical model for multiple well cases for CO_2 sequestration in saline formations.

3.6.2 Pressure profile for Multiple well

In order to model the analytical model for multiple well cases in an infinite acting formation, the pressure profile is examined. The theory of pressure transient analysis is similar to the theory of heat transfer in solids. For infinite acting multiple well systems in oil fields, pressure transient analysis is already done using the superposition principle. Mathematically, the superposition principle states [56] that the linear combinations of particular solutions to a linear and homogeneous differential equation is a solution to the differential equations (in our case equations are not linear and validation should be made for each case). This technique uses the summation of the particular solutions by treating one boundary equation at a time [57].

$$P_{final} = P_i + \sum_{n=1}^{n} P_n, \tag{3.37}$$

where n represents the number of injection wells.

Thus, we implemented the superposition technique to develop our new multi-well injectivity analytical model for predicting the pressure at any point in the formation for CO_2 storage in saline aquifers. We used the analytical model for single well case scenarios for prediction of pressure build-up in saline aquifers developed by [39]. Now, using this analytical model and superposition technique, we developed analytical model for multiple well scenarios for CO_2 sequestration in saline aquifers. Thus, we concluded that as we increase the number of wells the total pressure build-up in the reservoir will be the total summation of pressure build-up due to each individual well [58]. Equation 3.37 is used for the estimation of pressure at any point during CO_2 storage in saline aquifer.

Now, we provided the model validation for our multiple well scenarios. We developed the analytical model for multiple well scenarios with radial extents for 6, 8 and 10 km. We considered the model domain with a square area of 200 km $\times$ 200 km. We applied the superposition principle to Equations 3.28, 3.29 and 3.30. Similar to the previous Section 3.5, we used the same fluid properties as provided in the Berkeley laboratory study. We compared our analytical model to the results obtained by Ghaderi et al. [54] numerical simulations for Berkeley study (refer Figure 3.8). It was observed that the results from the analytical modeling for multiple well scenarios are in close agreement with the one

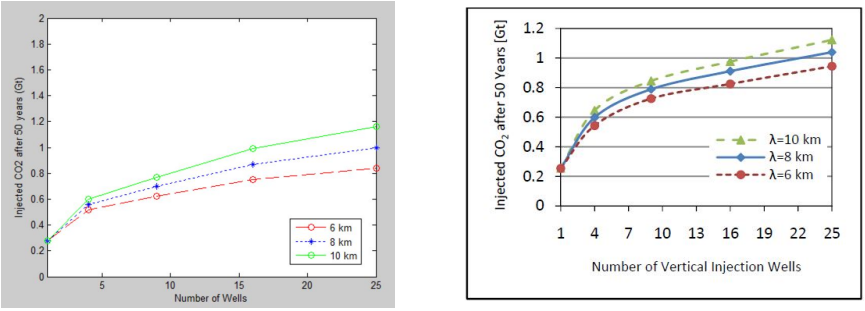

(a) Analytical result. (b) Numerical result.

Figure 3.8: Variation of injected CO_2 versus number of wells and distance between them.

Amount of CO_2 injected Gt for 50 years						
	Analytical Model			**Numerical Model**		
Number of Wells	6km	8km	10km	6km	8km	10km
1	0.28	0.28	0.28	0.25	0.25	0.25
4	0.52	0.56	0.6	0.55	0.6	0.65
9	0.62	0.7	0.77	0.75	0.8	0.85
16	0.75	0.87	0.99	0.82	0.9	0.95
25	0.84	1	1.16	0.92	1	1.1

Table 3.3: Table showing analytical and numerical modeling parameters used for variation of injected CO_2 versus number of wells and distance between wells.

obtained from the numerical modeling. Thus, now we can move forward and use it for optimizing the injection capacity of a potential CO_2 storage site to maximize the amount of CO_2 in saline formation.

3.7 Sensitivity Analysis

In this section, the sensitivity analysis for various input parameters during analytical modeling is examined. There are several parameters such as reservoir thickness, permeability and compressibility which affect the reservoir pressure during injection of CO_2 in saline formation. The determination of pressure build-up during injection is difficult because the pressure value changes due to the effect of these parameters. Thus, the sensitivity

analysis was carried out to investigate the effect of these parameters on the amount of CO_2 injected and stored after 50 years. All these parameters were chosen closer to the reservoir properties. Figure 3.9, 3.10 and 3.11 shows the sensitivity analysis of each of these parameters. All these parameters were compared to numerical simulations results obtained by Ghaderi et al. [54].

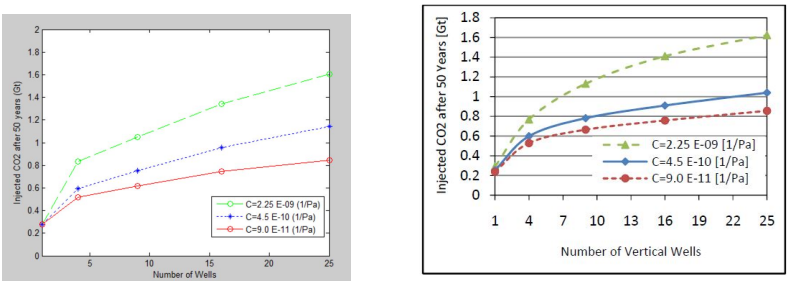

(a) Analytical result. (b) Numerical result.

Figure 3.9: Effect of Compressibility on storage capacity.

The most important parameter which effects the storage capacity is Compressibility. During the sensitivity analysis, the value of compressibility was varied from 2.25×10^{-9} to $9 \times 10^{-11}(1/\text{Pa})$. We concluded that rocks with lower compressibility will have higher storage capacity (refer to Figure 3.9). We also noted that higher value of compressibility increases the storage capacity when we increase the number of wells.

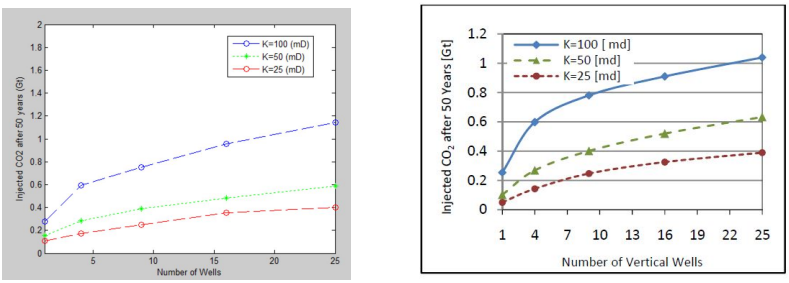

(a) Analytical result. (b) Numerical result.

Figure 3.10: Effect of Permeability on storage capacity.

The second important parameter which we saw that effect the storage capacity is Permeability. During the sensitivity analysis, the value of permeability was varied from 25 to 100mD. We concluded that higher value of permeability will have higher storage

capacity (refer to Figure 3.10). We also noted that by reducing the permeability to 25mD, the amount of CO_2 stored is reduced tremendously. It was also observed that by increasing number of wells, the effect of permeability on storage capacity is low.

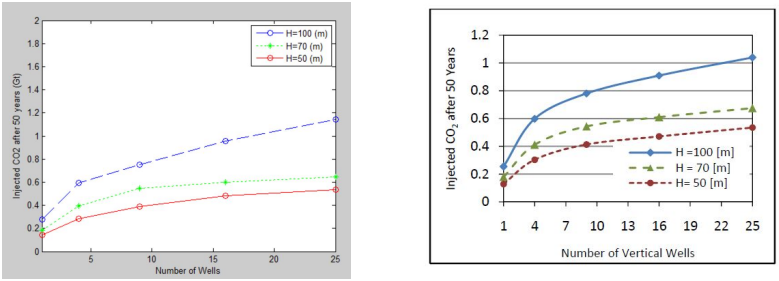

(a) Analytical result. (b) Numerical result.

Figure 3.11: Effect of Thickness on storage capacity.

The last parameter which we saw that effect the storage capacity is Formation Thickness. During the sensitivity analysis, the value of thickness was varied from 50 to 100m. We concluded that lower value of thickness will have storage capacity decreased by 50 percent as seen in Figure 3.11. It was also observed that by increasing number of wells, the effect of thickness on storage capacity is high.

3.8 Modeling Brine injection (Single Phase flow)

For the modeling of brine production we move forward with the single phase model. A single phase flow model is a model where single fluid exist *i.e.* Pure Brine injected in a brine reservoir. There are many assumptions made to simplify the problem for analytical model in single phase flow. The model is assumed to be homogeneous, infinite acting, isothermal, isotropic and horizontal. Reservoir compressibility, thickness, fluid viscosities are all kept constant. The well is centered in a cylindrical reservoir with a wellbore radius of flow r_w. There is no flow across the outer boundary. The effect of capillary, gravity and skin factor are neglected for simplicity.

We used constant-terminal-rate solution for single phase model to predict the pressure buildup analysis for single well at constant rate proposed by Mathews and Russell [58].

$$P_w = P_i + \frac{70.6 q_{CO_2} \mu B_g}{kh} E_i\left(\frac{-948 \phi \mu c_{ti} r_w^2}{kt}\right). \tag{3.38}$$

The mathematical function E_i is defined as Exponential Integral and is given by:

$$E_i(-x) = -\int_x^{\infty} \frac{e^{-u}du}{u} = \Big[\ln x + \sum_{i=1}^{\inf} \frac{(-1)^x}{x!}\Big]. \tag{3.39}$$

Equation 3.38 is for a Single phase analytical model and is used to determine pressure build-up for single well brine production from a brine reservoir.

3.9 Summary

In this chapter we gave an introduction to single well analytical modeling to determine the pressure build-up during CO_2 injection in Section 3.3 by going over the various analytical models for single well scenarios. We went through various approaches for determination of saturation fronts in Section 3.4 which are often implemented for determination of pressure profile during injection. We however showed in Section 3.5 the analytical model we used to validate reservoir pressure for single well modeling using Berkeley study as an example. In Section 3.6 we commented on analytical modeling for multiple well scenarios. We also discussed how pressure profile was developed for multiple well scenarios using superposition principle. We presented sensitivity analysis for significant parameters during analytical modeling. Finally, in Section 3.8 we presented analytical single phase modeling for production of brine from saline formations.

The following Chapter present four case scenarios for single well and multiple well modeling for infinite acting formation while accounting for important parameters such as relative permeability and well interference. We also presented the results obtained during optimization of injection capacity for CO_2 in saline formations.

Chapter 4

Results and Discussions

In this chapter, we present the single well solutions developed in the previous chapters for different reservoirs. The model is assumed for CO_2 injection in a homogeneous, horizontal and infinite acting saline formation. The solutions are presented for Viking aquifer, Michigan basin, Nisku aquifer and Mount Simon sandstone. A comparison with numerical simulations is also presented to validate our analytical model. We also did optimization to increase the injection capacity of CO_2 in saline aquifer.

4.1 Single Well Modeling

4.1.1 Single Well Case Study 1 - Viking Aquifer in the Alberta Basin

The Alberta Sedimentary basin in western Canada is considered as one of the largest petroleum producers in the world. The Alberta basin is well suited for CO_2 sequestration as it meets all reservoir scale criteria such as favorable geology and hydrogeology, available oil and gas reservoirs and tectonic stability [21]. This basin contains sandstone and carbonates which forms the aquifer. Out of these aquifer, Viking aquifer was considered to be one of the dominant aquifer for the determination of injection capacity in saline formations. We use the Viking aquifer reservoir field example from Burton et al. [35] for our work. Table 4.1 lists all the reservoir parameters used for modeling of CO_2 in saline formations. According to the data, initial pressure is 1800psi and maximum reservoir pressure is 2800psi. This aquifer was assumed to be homogeneous, isotropic, infinite-acting formation, gravity and

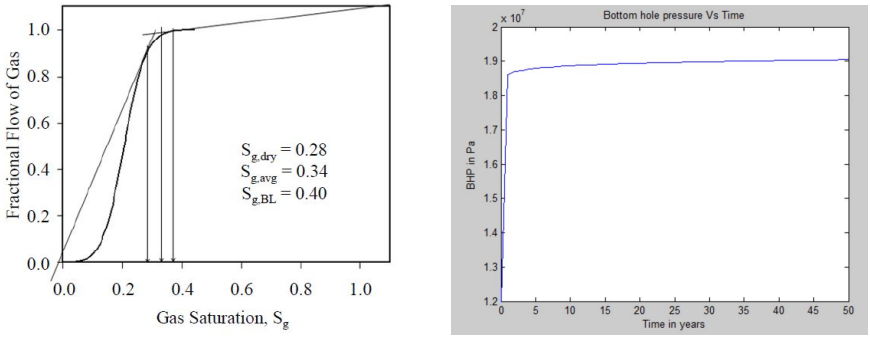

(a) Fractional flow curve. (b) Pressure build-up profile.

Figure 4.1: Fractional flow and pressure profile for Viking aquifer.

Parameters	**Value**
Porosity (ϕ)	0.135
Permeability (k)	30 mD
Thickness (h)	40 m
Brine Viscosity (μ_w)	0.7 cP
CO_2 Viscosity (μ_g)	0.17 cP
Rock Compressibility (c_r)	1.45×10^{-10} 1/Pa
Brine Compressibility (c_w)	1×10^{-9} 1/Pa
Gas Formation Volume Factor (B_g)	0.003 rB/SCF
Injection Rate (Q)	2.47 m^3/s
Time (t)	50 years
Radius of well (r_w)	0.076 m
Initial Pressure (P_i)	1.241×10^7 Pa
Fracture Pressure (P_f)	1.931×10^7 Pa
Gas saturation of dry front (S_{gdry})	0.28
Gas saturation of BL front (S_{gBL})	0.40
Average saturation front (S_{avg})	0.34

Table 4.1: Reservoir parameters used for modeling in the Viking Aquifer.

injection was simulated as one-dimensional radial flow at a constant injection rate. We used the relative permeability data reported for Viking sandstone by Bennion and Bachu [59].

For the calculation of saturation fronts ($i.e.$ S_{gBL} and S_{gdry}), we used the results obtained by [35] using the Noh et al. [42] approach. In our case, average saturation front (S_{avg}) is 0.34 as shown in Figure 4.1(a). Once the accurate saturation fronts are determined,

all the analytical model parameters can be determined and the analytical two phase model can be run. Figure 4.1(b) shows pressure build-up for single well CO_2 injection in saline formations. In our case, maximum BHP reaches 1.938×10^7Pa implying that our analytical model is valid as the maximum BHP obtained by numerical simulator is 1.931×10^7Pa.

4.1.2 Single Well Case Study 2 - Bass Islands Dolomite in the Michigan Basin

The Midwest Regional Carbon Sequestration Project Partnership (MRCSP) has conducted CO_2 injection test at Otsego County, Michigan in the Bass Islands Dolomite saline formation. The formations are at the depth of 1049-1071m. According to [60], the rock test suggested an average permeability of 22mD, porosity of 13% and the net thickness of the aquifer is 200m, initial pressure of 1.05MPa and fracture pressure 1.38MPa. In this study, this aquifer was assumed to be homogeneous, isotropic, infinite-acting formation and injection was simulated as one-dimensional radial flow at a constant injection rate.

Parameters	**Value**
Porosity (ϕ)	0.13
Permeability (k)	22 mD
Thickness (h)	200 m
Brine Viscosity (μ_w)	0.7 cP
CO_2 Viscosity (μ_g)	0.17 cP
Rock Compressibility (c_r)	1.45×10^{-10} 1/Pa
Brine Compressibility (c_w)	1×10^{-9} 1/Pa
Gas Formation Volume Factor (B_g)	0.003 rB/SCF
Injection Rate (Q)	6.5 m^3/s
Time (t)	50 years
Radius of well (r_w)	0.076 m
Initial Pressure (P_i)	1.05×10^7 Pa
Fracture Pressure (P_f)	1.38×10^7 Pa
Gas saturation of dry front (S_{gdry})	0.26
Gas saturation of BL front (S_{gBL})	0.34
Average saturation front (S_{avg})	0.3

Table 4.2: Parameters used for modeling in Michigan Basin.

The main aim of this project is to inject 10,000 metric tons of CO_2 in saline formations for the evaluation of CO_2 sequestration potential for Michigan Basin. In 2006, a test well named, *State−Charlton 4-30* was drilled and this was done for monitoring of injection well.

At the start of injection, 450 metric ton of CO_2 was injected per day. The BHP recorded was around 13,800kPa. The input parameters used to calculate the pressure build-up are listed as seen in Table 4.2.

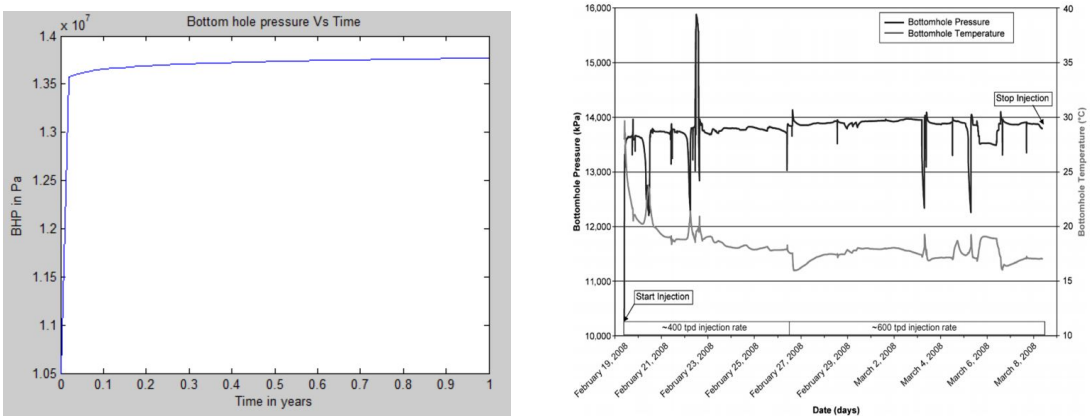

(a) Analytical Modeling. (b) Numerical Modeling.

Figure 4.2: Comparison of Analytical model of Michigan Basin with Numerical simulations.

Using the reservoir parameters, we used our analytical model to determine the reservoir pressure during the injection test. Then, the analytical model for single well scenarios were compared with numerical modeling for validation purpose. We used the simulation result obtained by Sminchak et al. [60]. Figure 4.2 shows the pressure build-up for single well CO_2 injection in saline formations. In our case, the maximum reservoir pressure reaches 1.38×10^7Pa which is similar to the result obtained by the numerical simulator ($i.e.$ 13,800kPa) implying that our analytical model is valid.

4.2 Multiple Well Modeling

4.2.1 Multiple Well Case Study 1 - Nisku Aquifer

According to the Alberta Geological Survey [61], Nisku formation in the southwest of Edmonton has been identified as the potential storage site for CO_2 sequestration in saline aquifer for a variety of favorable conditions such as capacity, confinement and injectivity. The project is examining the feasibility to store 20 Mt CO_2 for time period of 50 years. According to [54], the net thickness of the aquifer is 102m, initial pressure is 16MPa and

fracture pressure is 36MPa. In this study, this aquifer was assumed to be homogeneous, isotropic, infinite-acting formation. The input parameters used to calculate the pressure build-up are listed as seen in the Table 4.3. We used the relative permeability data given in [59].

Parameters	**Value**
Porosity (ϕ)	0.064
Permeability (k)	46 mD
Thickness (h)	102 m
Brine Viscosity (μ_w)	0.84 cP
CO_2 Viscosity (μ_g)	0.062 cP
Rock Compressibility (c_r)	1.45×10^{-10} 1/Pa
Brine Compressibility (c_w)	1×10^{-9} 1/Pa
Gas Formation Volume Factor (B_g)	0.003 rB/SCF
Injection Rate (Q)	17.01 m^3/s
Time (t)	50 years
Radius of well (r_w)	0.076 m
Initial Pressure (P_i)	1.6×10^7 Pa
Fracture Pressure (P_f)	3.1×10^7 Pa
Relative Permeability Data	
Brine residual saturation (S_{wr})	0.423
CO_2 residual saturation (S_{gr})	0
Brine relative permeability component (n)	3
CO_2 relative permeability component (m)	3
CO_2 endpoint relative permeability (k_{rg0})	0.099
Brine endpoint relative permeability (k_{rw0})	1

Table 4.3: Parameters used for modeling in Nisku Aquifer.

Approach	S_{gBL}	S_{gdry}	S_{avg}	**Maximum BHP**
Noh et al.[42]	0.32	0.465	0.4	29 MPa
Woods et al.[44]	0.33	0.58	0.46	28.5 MPa
Welge [43]			0.43	34 MPa
CMG Numerical Model				31 MPa
Analytical Model			0.41	31.2 MPa

Table 4.4: Determination of average saturation fronts by various graphical approach.

We evaluated two saturation fronts using all the different approaches to compare our results (refer to Table 4.4). Table shows how the maximum reservoir pressure changes with different value of average saturation fronts (S_{avg}) emphasizing the importance of validating

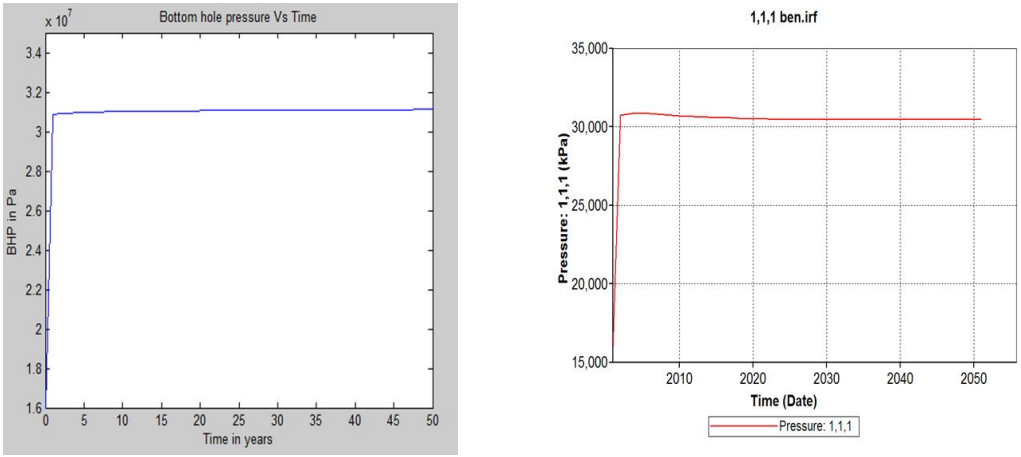

(a) Analytical Modeling.

(b) Numerical Modeling.

Figure 4.3: Comparison of analytical model of Nisku Aquifer with numerical simulations.

the model before using it to perform further analysis. As we know the saturation front is very sensitive to the reservoir pressure in order to get a better estimation of the saturation front, we used modified Welge tangent approach. For Mount Simon sandstone using our approach, we get the value of average saturation front (S_{avg}) to be 0.41 for Nisku aquifer. The pressure build-up was found to be 31.2MPa which is in closer agreement with the numerical model ($i.e.$ 31MPa).

After the prediction of saturation fronts, the rise in reservoir pressure due to injection of CO_2 can easily be determined. The analytical model for single well scenarios are compared with numerical modeling for validation purpose. We used numerical simulation result obtained by [54]. Figure 4.3 shows pressure build-up for single well CO_2 injection in saline formations. In Nisku formation, the fracture pressure is approximately 36MPa and the pressure is kept below fracture pressure 32MPa ($i.e.$ 90% of 36MPa). In our case, the reservoir pressure reaches 3.1×10^7Pa which is similar to the result obtained by the numerical simulator ($i.e.$ 31,000kPa).

Now, we extend our analytical model from a single well scenario to multiple well scenarios with the help of superposition principle. Using this principle, we developed an analytical model for 20 injection well scenarios. We considered the model domain with a square area of 20 km$\times$20 km. Once modeled, the analytical solutions were compared with numerical model. To validate our model, we used the numerical simulation results obtained for Nisku formation by [54]. Figure 4.4 shows the comparison of analytical model

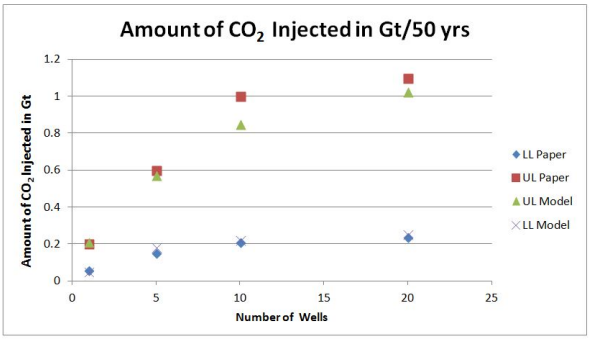

Figure 4.4: Variation of Nisku capacity with respect to number of wells. *LL* represents Lower Limit and *UL* represents Upper Limit.

with numerical model for 20 wells after 50 years of injection. In the results shown in figure 4.4, blue and white points present the injection capacity of the focus area with the following reservoir properties: porosity 20%, permeability 90mD and rock compressibility of $1.45\times10^{-9}(1/\text{Pa})$; whereas red and green points represent the base case properties such as porosity 10%, permeability 50mD and rock compressibility of $9\times10^{-11}(1/\text{Pa})$. Thus it was observed that results obtained by the numerical simulator are in close agreement with the analytical model implying that our analytical model for multiple well scenarios is valid.

4.2.2 Multiple Well Case Study 2 - Mount Simon Sandstone

The Midwest Geological Sequestration Consortium (MGSC) [62] was found to predict the long term storage of CO_2 in the Mount Simon sandstone near the Illinois basin. The Mount Simon Sandstone is a saline water filled aquifer and is considered as one of the potential site for geological sequestration. This project is most commonly known as Illinois Basin Decatur Project (IBDP).

The project is injecting 100 Mt of CO_2 for 50 years into the Mount Simon Sandstone. The project simulated CO_2 injection with an injection rate of 5 Mt/year/well with 20 number of wells. The aquifer has 10% porosity, permeability ranges from 1.4×10^{-18} to $6.7\times10^{-20}m^2$ and rock compressibility ranges from 3.7×10^{-10} to $6.0\times10^{-10}Pa^{-1}$ and the thickness of Mount Simon sandstone varies from 300 to 700m [31]. The assumptions for IBDP are infinite acting boundary conditions, homogeneous and isotropic [63]. The input parameters used to calculate the pressure build-up are listed as seen in the Table 4.5.

We modeled the relative permeability curve for Mount Simon sandstone aquifer us-

Parameters	**Value**
Porosity (ϕ)	0.1
Permeability (k)	5 mD
Thickness (h)	500 m
Brine Viscosity (μ_w)	0.84 cP
CO_2 Viscosity (μ_g)	0.07 cP
Rock Compressibility (c_r)	3.71×10^{-10} 1/Pa
Brine Compressibility (c_w)	1×10^{-9} 1/Pa
Gas Formation Volume Factor (B_g)	0.011 rB/SCF
Injection Rate (Q)	85.26 m^3/s
Time (t)	50 years
Radius of well (r_w)	0.076 m
Initial Pressure (P_i)	1.5×10^7 Pa
Fracture Pressure (P_f)	2.7×10^7 Pa
Relative Permeability Data	
Brine residual saturation (S_{wr})	0.34
CO_2 residual saturation (S_{gr})	0
Brine relative permeability component (n)	3
CO_2 relative permeability component (m)	3
CO_2 endpoint relative permeability (k_{rg0})	0.0
Brine endpoint relative permeability (k_{rw0})	1

Table 4.5: Parameters used for modeling in Mount Simon Sandstone.

Approach	S_{gBL}	S_{gdry}	S_{avg}	**Maximum BHP**
Noh et al.[42]	0.3	0.41	0.36	22 MPa
Woods et al.[44]	0.32	0.5	0.41	21.2 MPa
Welge [43]			0.38	23 MPa
CMG Numerical Model				24.3 MPa
Analytical Model			0.35	24 MPa

Table 4.6: Determination of Average Saturation Fronts by various graphical approach.

ing the data reported in [64]. We evaluated two saturation fronts using all the different approaches to compare our results (refer to Table 4.6). Table shows how maximum BHP changes with different value of average saturation fronts (S_{avg}). We used modified Welge tangent approach for determining the average saturation front for Nisku aquifer. Using our approach, we get the value of average saturation front (S_{avg}) to be 0.35 for Mount Simon sandstone. The pressure build-up was found to be 24MPa which is in closer agreement with the numerical model ($i.e.$ 24.3MPa).

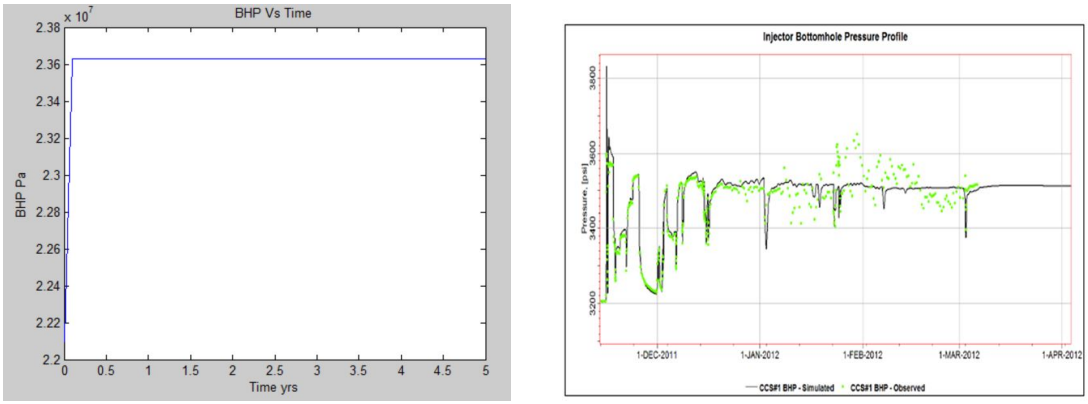

(a) Analytical Modeling. (b) Numerical Modeling.

Figure 4.5: Comparison of Analytical model of IBDP with Numerical simulations.

After the prediction of saturation fronts, the rise in BHP due to injection of CO_2 can easily be determined. The analytical model for single well scenarios are compared with numerical modeling. In this model, ECLIPSE 300 (v2011.2) reservoir simulator is used to validate the model. Figure 4.5 shows pressure build-up for single well CO_2 injection in saline formations. In Mount Simon sandstone saline formation, the fracture pressure is approximately 27MPa and the pressure is kept below fracture pressure 24.3MPa (*i.e.* 90% of 27MPa). In our case, reservoir pressure reaches 2.43×10^7Pa which is similar to the result obtained by the numerical simulator [65] (*i.e.* 3560psi).

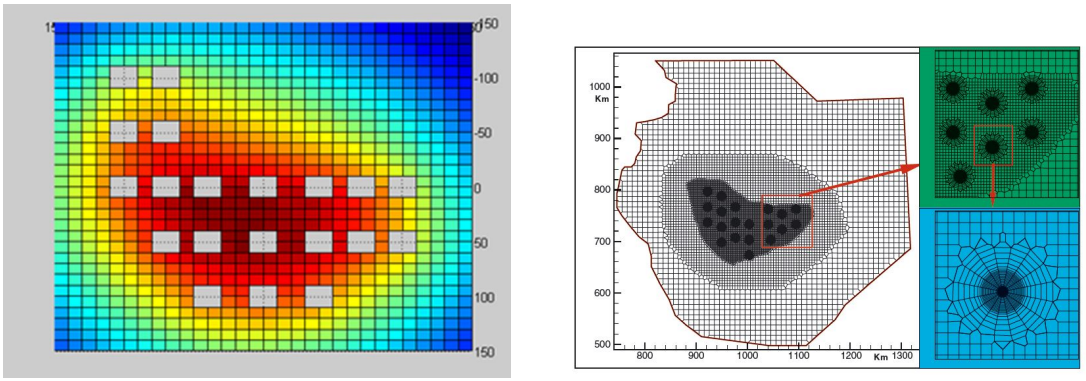

(a) Analytical Modeling. (b) Numerical Modeling.

Figure 4.6: Comparison of Analytical model of IBDP with Numerical simulations for 20 injection wells.

Now, we extended our analytical model from a single well scenario to multiple well scenario with the help of superposition principle. Using this principle, we developed analytical model for 20 injection well scenarios with 10km spacing. We considered the model domain with a square area of 27 km×30 km. Once modeled, the analytical solutions are compared with numerical model. To validated our model, we used the numerical simulation results obtained by Zhou et al. [66]. Figure 4.6 shows the comparison of analytical model with numerical model for radial extent of 10km after 50 years of injection. Thus it is observed that results obtained by the numerical simulator are in close agreement with analytical model implying that our analytical model for multiple well scenarios is valid.

4.3 Optimization of Multiple wells

In order to make carbon sequestration in saline formations a viable option to tackle climate change, we should be able to sequester large quantities of CO_2 for which we need to have a sufficiently large aquifer with high reservoir thickness, porosity and permeability but lower reservoir compressibility in order to keep the reservoir pressure below the fracture pressure. The second part of thesis focuses on optimizing the amount of CO_2 sequestered into the saline aquifer which is said to be build on the elementary optimization of placement of wells done by Joshi [40]. We try increasing the storage capacity of a potential site by looking at different optimization parameters as listed below.

- Optimization of injection wells,
- Optimization of injection flow-rate,
- Optimization of reservoir pressure using relief wells.

4.3.1 Optimization of Injection Wells

We are required to inject the maximum amount of CO_2 within a relatively small area for a short period of time but on doing so there is an exponential increase in reservoir pressure. It is important to maintain reservoir pressure below the fracture pressure either by having low injection rates or by increasing the injection period, both of which are undesirable.

One way to increase the sequestration capacity by maintaining the same injection rate and injection time period is by using the multiple well injection strategy $i.e.$ to drill as many injection wells so as to cover the maximum available pore space within a short period

of time. By using multiple well strategy, the injection rate per well can be maintained low as the total CO_2 injection rate is split equally among the various injection wells.

In the study, we try injecting CO_2 for different well scenarios with the constraint of maintaining the reservoir pressure under 90% of the fracture pressure during the injection period. We used the reservoir parameters used in Berkeley Laboratory study as listed in Table 3.1. The numbers of wells were systematically increased from 1 to 4 to 5 to 8 to 9 to 13 to 16 to 24 and finally to 25 keeping the distance between the wells close to 10km as shown in Figure 4.7. It was safe to consider this distance as the rise in the plume of CO_2 for each well system was found out to be within 5km [67].

It was observed that as we increase the number of wells, the amount of CO_2 injection capacity increases. This is because as we increase the number of wells we get more available pore space leading to increase in the pore volume available for CO_2 storage. But increasing the number of wells may not be economically feasible, as each well cost around millions of dollars. In order to optimize the number of wells, we look at variable scenarios of well placement.

In the next approach we tried by optimizing the placement of wells randomly. This was done by trial and error approach at first as seen in the Figure 4.8 and then was perfected using the optimizing tool such as genetic algorithm. During this approach, we found that symmetrical placed wells are the one which gives better result compared to unsymmetrical pattern. We also found that when the injection area is kept constant the injection capacity of the reservoir increases with the increase in the number of wells at first but later it tapers down. This behavior is due to the fact that as we increase the number of wells, we are able to access more and more available pore volume until there are no more extra pore spaces.

The other major observation we found here was the maximum pressure build-up occurs in the center of the reservoir as seen in the Figure 4.9. This happens due to the superposition principle, which occurs due to the fact that in case of ideal reservoir conditions a group of wells when looked upon from a distance will act in a similar way to one large well placed at the center of the wells.

Next approach to optimize the well placement was to lower the pressure build-up in the reservoir by removing the well in the middle. So, we optimized the wells from 5 to 4 wells, from 9 to 8 wells and from 25 to 24 wells. On decreasing the wells from 5 to 4, we found that the wells did not interact that much and the pressure rises in the middle well was not that high due to other wells. But on removing a well in case of 9 to 8 wells and from 25 to 24 wells, it was seen that the amount of CO_2 injected increased by around 3.5% in both the cases (3.8% and 3.2% respectively). Next approach we implemented was

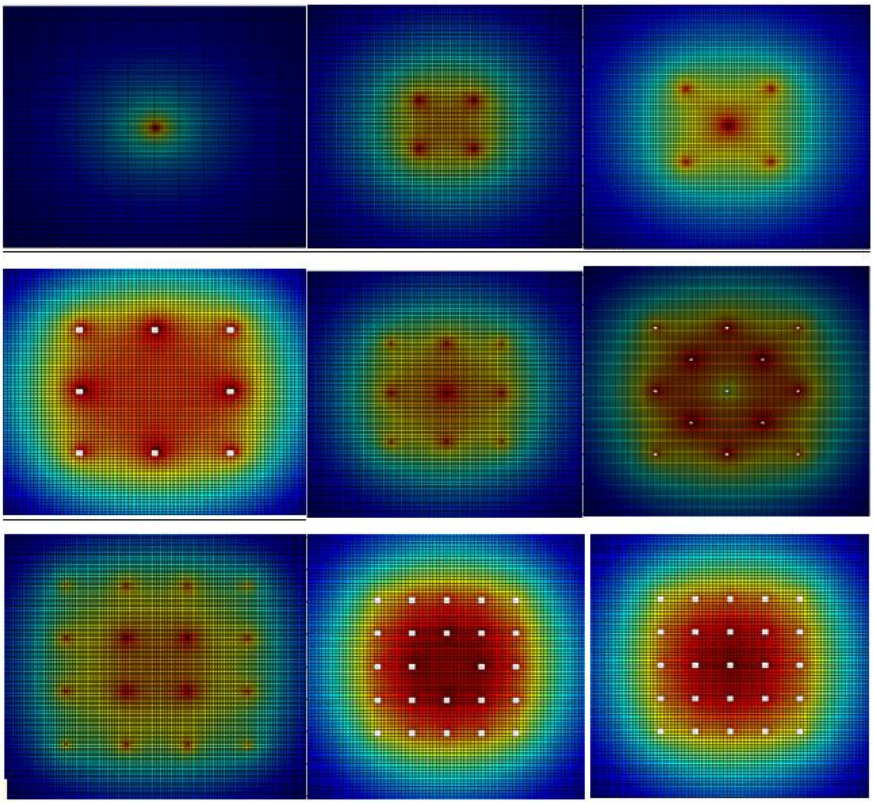

Figure 4.7: Well placement for multiple wells (*1*, *4*, *5*, *8*, *9*, *13*, *16*, *24 and 25*).

by removing bunch of wells 16 to 12 wells and from 25 to 16 wells. It was seen that the amount of CO_2 injected increased by 3.6% to 5% respectively. Thus, by decreasing the number of well we are able to increase the injection capacity of the reservoir.

Then, we tried optimizing by keeping the same number of well but changing the well positions. It was observed that for increasing the sequestration capacity it was important to keep the wells as far as possible to prevent pressure build-up. This can be achieved by placing the well on the boundary of the injection area. For example, in case of 16 boundary wells we found that we are able to sequester 5% more CO_2 than for 25 wells. Similarly, by placing the 8, 9, 16 or 25 wells at the boundary we get higher sequestration. There are various other comparisons done as shown in the Table 4.7 to get the optimized wells and it was noted that using 12 wells will give good optimization considering the cost but 24 wells give maximum amount of sequestration about 0.96 Gt for a period of 50 years of injection.

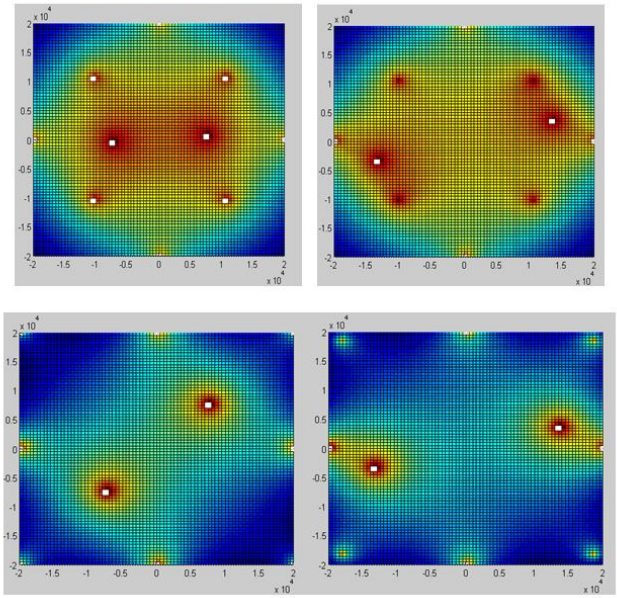

Figure 4.8: Optimization of well placement (*for 10 wells*).

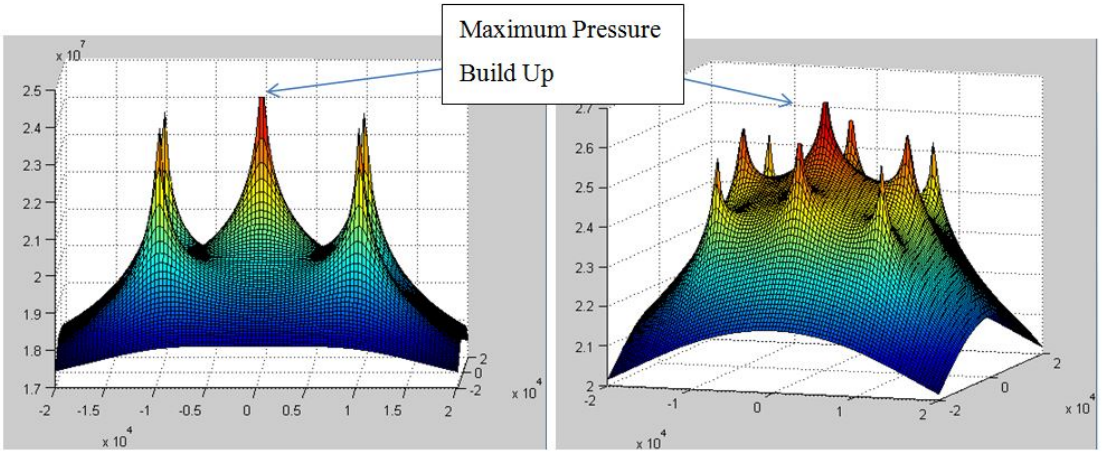

Figure 4.9: Showing maximum pressure build up at the centre.

Number of Wells	**Injection Capacity** (Gt CO_2/ 50 years)
1	0.28
4	0.52
5	0.58
8	0.70
9	0.68
12(Circular)	0.77
12(Boundary)	0.84
16	0.81
16(Boundary)	0.92
24	0.92
25	0.89

Table 4.7: Showing the increase in the amount CO_2 injected for different types of well arrangement.

4.3.2 Optimization of Injection Flow-rate

The next approach that we followed was using Continuous Cyclic CO_2 injection (CCCI) Method. On injecting CO_2 continuously, we were able to inject about 7×10^6 m^3/day. On doing so we were able to reach the fracture pressure of 27MPa in about a year time period. For this case study we tried injecting 6×10^6 m^3/day CO_2 for a certain period of time (10 years) and then as soon we reach the reservoir pressure of about 25MPa in a year time. We then close the injection well and wait for the pressure to decrease to around the initial reservoir pressure due to pressure dissipation. After 10 years we again start the injection process. The overall total injection capacity of the reservoir is got by multiplying the injection rate with the time period the well is actively injection which in this case is 30 years (10×3). The overall injection capacity without CCCI and with CCCI is about 0.25 Gt and 0.15 Gt respectively. It was noted that for a cyclic period of 10 years the using CCCI is not beneficial.

Next we tried using CCCI with different cyclic time. It was seen that as we decrease the cyclic time from 10 to 5 years, we were able to see an increase in the injection capacity, but the overall injection was less than the injection capacity of the site when compared to it being operated without CCCI. As there is no improvement in the CO_2 sequestration capacity of the site, we do not pursue this approach.

The next part of the thesis revolves around increasing the injection capacity of a reservoir by optimizing the injection flow-rate through each well. The previous section

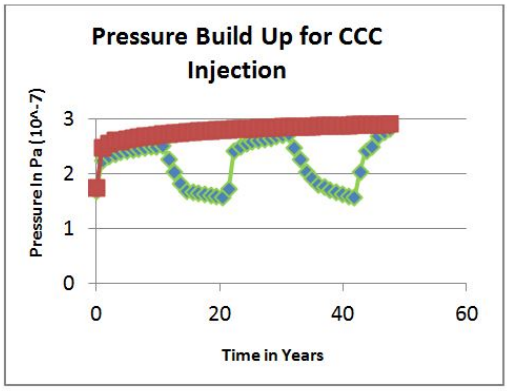

(a) Analytical Model.

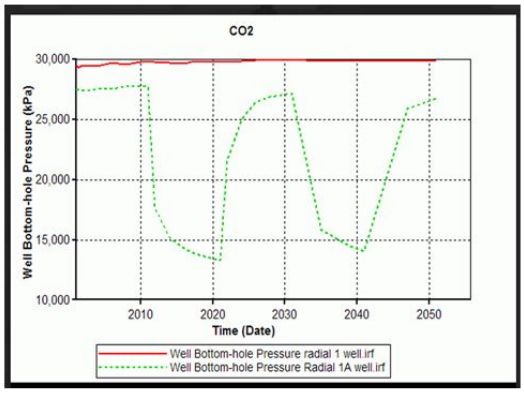

(b) Numerical Model.

Figure 4.10: Comparison of Analytical model with Numerical simulations.

focused on optimization by increasing the number of wells and it concluded that the maximum pressure build-up happens at the center of the reservoir. Considering this fact, we carry out simulations so as to inject more amount CO_2 at the boundary and less at the center to compensate for the pressure rise at the center.

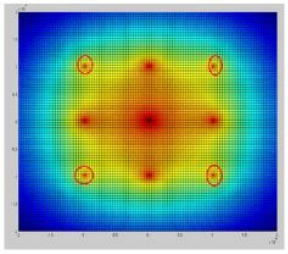

(a) 9 wells.

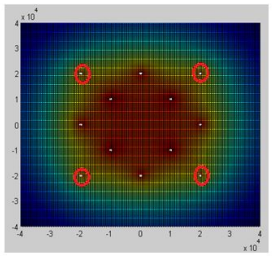

(b) 12 wells.

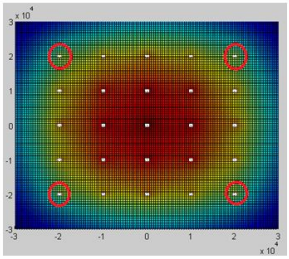

(c) 25 wells.

Figure 4.11: Wells shown by red circles indicates wells with higher flow-rates.

Until now, simulations were carried out using the same injection flow-rate in each well constant (For example, for 9 wells individual flow-rate will be $Q/9$). Now, we try changing the flow-rates in different wells. For initial analysis, two flow-rates were considered Q_1 and Q_2 where $Q_1 < Q_2$. Q_2 was injected at the boundary wells (*highlighted in red*) as shown in the Figure 4.11 and the other wells were injected with the flow-rate Q_1.

Thus, we concluded that CO_2 injection capacity of the reservoir increased when

flow-rate was increased. This observation can be explained on ideal infinite acting reservoir theory. As the reservoir is ideal and homogeneous, so the pressure build-up at the boundary is symmetrical and is distributed evenly across the reservoir. So using variable flow-rate technique, we prevent higher pressure build-up at the center thereby, keeping the reservoir integrity intact. It was also noted that the effect of varying the flow rate on the injection capacity of the reservoir is not very significant for higher number of wells.

The analysis shows that there is not a significant increase in the injection capacity of the reservoir for higher number of wells as the sequestration difference is less than 2% for these cases. This can be concluded that as we increase the number of wells it increases the number of available pores inside the reservoir. As most of the pore volumes are already saturated as we reach higher number of wells so varying the flow-rate does not have a significant effect on the storage capacity as seen in the Table 4.8. Thus, changing the flow-rates and maintaining different flow-rates for the entire injection wells is not that economical and practical for a real case scenario.

Amount of CO_2 injected (Gt CO_2 for 50 years)			
	Constant Flow rate	**Variable Flow rate**	**Percentage Increase**
Wells			
9	0.68	0.76	11.57
12	0.84	0.89	7.05
16	0.81	0.82	1.23
25	0.89	0.90	1.04

Table 4.8: Showing the amount of CO_2 injected for different numbers of wells based on flow-rates.

4.3.3 Optimization of reservoir pressure using relief wells

According to [68], it was suggested that one of the ways to maintain the reservoir pressure below fracture pressure is by the placement of relief wells. As we are mainly focusing on one of the ways to decrease the pressure inside the reservoir during CO_2 sequestration in saline aquifer, we optimized production wells so as to produce brine from the reservoir. The approach is done by assuming Single Phase flow model as seen in Section 3.8.

The single phase model approach adopted in our work requires less input parameters and less specialized technical knowledge as it considers brine production by a brine reservoir similar to water production by a water well. The assumptions are very simple

Parameters	Value
Porosity (ϕ)	0.12
Permeability (k)	100 mD
Thickness (h)	100 m
Viscosity (μ)	0.25 cP
Compressibility (c_{ti})	3.3×10^{-6} 1/psi
Gas Formation Volume Factor (B_g)	1.075 rB/SCF
Injection Rate (Q)	0.2 Gt/years
Time (t)	50 years
Radius of well (r_w)	0.076 m
Initial Pressure (P_i	1740 psi
Fracture Pressure (P_f)	4370 psi

Table 4.9: Parameters used for modeling Single-Phase Flow.

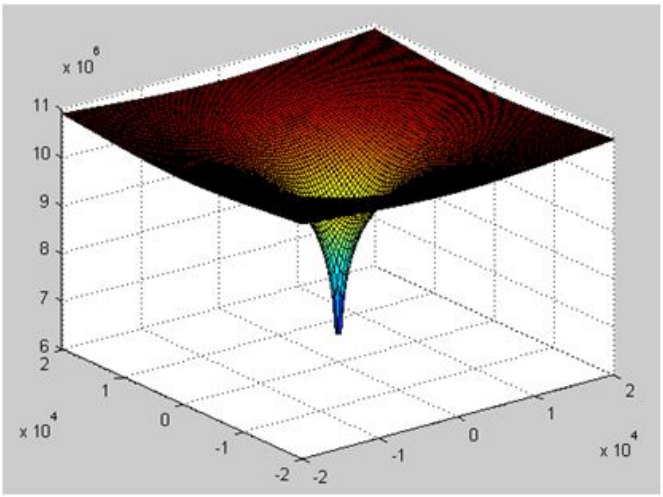

Figure 4.12: 3D Plot for reservoir pressure vs. Time for 50 years of Brine production.

and one dimensional radial flow for brine production is used. The model is assumed to be homogeneous, infinite acting, isotropic and horizontal. Reservoir compressibility, thickness, fluid viscosities are all kept constant. The well is centered in a cylindrical reservoir with a wellbore radius r_w. The effect of capillary, gravity and skin factor are neglected for simplicity. We considered the model domain within a square area of 200 km $\times$ 200 km. The aquifer is assumed to be fully brine saturated and has isothermal conditions with reservoir temperature at 45^0C. We have used general parameters as listed in Table 4.3.3

to develop the analytical model for production of brine as seen in Figure 4.12. Now, we extended our analytical model from a single well scenario to multiple wells scenario with the help of superposition principle mentioned previously in Section 3.6.2.

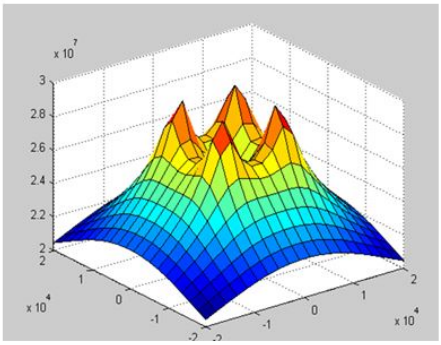

(a) 4 wells.

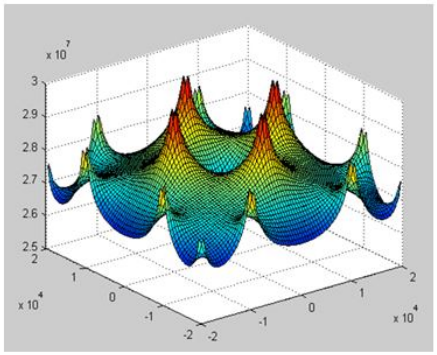

(b) 16 wells.

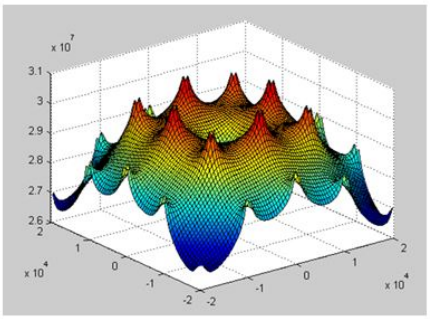

(c) 25 wells.

Figure 4.13: Wells showing the various injection well scenarios with one production well.

For this approach, we try by using one production well with various injecting wells as show in the Table 4.10. The production well was placed in the center of the reservoir to decrease the pressure build-up. It was seen that using production well along with injection wells we see that there is an increase in the total CO_2 storage capacity of the reservoir (refer to Figure 4.14).

This was due to the fact that increase in the reservoir pressure was counter balanced with the loss in the reservoir pressure due to brine production. This is similar to the way the reservoir pressure decreases due to oil and gas production. As it was seen from the Table 4.10 that having one production well goes a long way in decreasing the reservoir

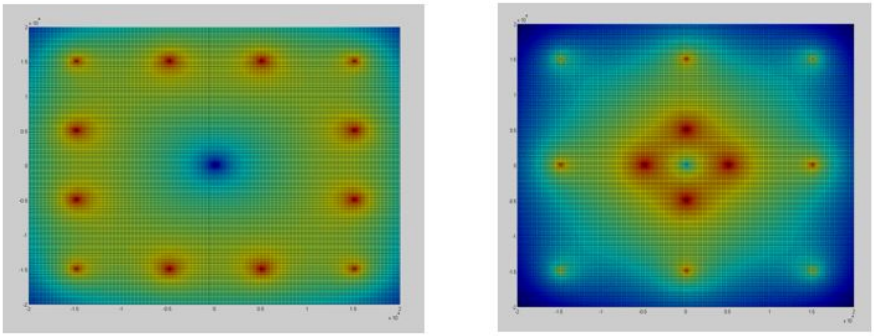

(a) 12 wells (*Boundary*). (b) 12 wells (*Circular*).

Figure 4.14: Well placement for 12 injection wells and 1 production well.

Comparison				
Number of wells		**Amount of CO_2 injected**		**Percentage increase**
Injection well	**Production well**	**With Production well**	**Without production well**	
8	1	0.72	0.70	2.08
12 (*Boundary*)	1	0.84	0.84	0.70
12 (*circle*)	1	0.78	0.76	2.71
16	1	0.82	0.81	1.82
24	1	0.94	0.92	1.59

Table 4.10: Showing the comparison of amount of CO_2 injected for different numbers of wells with and without a production well.

pressure, the next part of the study focused on using multiple production wells along with various injection well scenarios.

The placement of the production wells were selected in such a way that we had the maximum effect on decreasing the reservoir pressure. As seen from the previous section, the maximum pressure is in the middle so we try using 4 production wells in the center seen in Figure 4.15.

Once the placement of the injection and productions wells were decided we start the simulations keeping the same previous assumptions. Two different well case scenarios

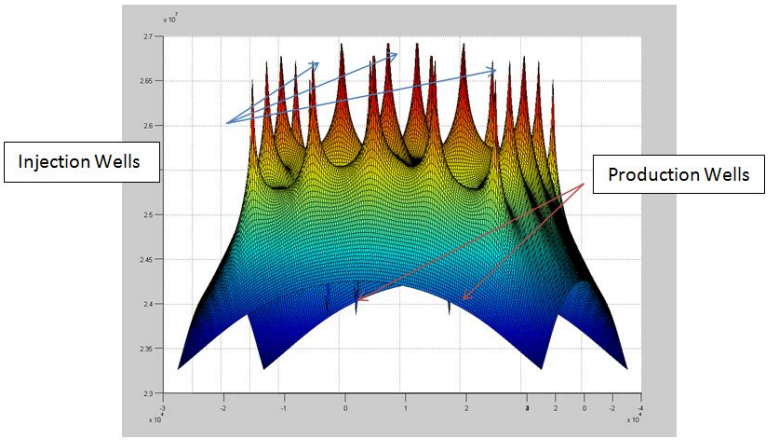

Figure 4.15: Placement of well: 20 injection well with 4 production well.

Comparison		
Number of wells		**Amount of CO_2 injected**
Injection well	**Production well**	Gt CO_2 for 50 yrs
9	4	0.72
13	4	0.84
16	5	0.78
17	5	0.82
17	5	0.82
20	5	0.94

Table 4.11: Showing the comparison of amount of CO_2 injected for different combination of injection and production wells.

were seen, first one with 13 wells and other one with 20 wells. Table 4.11 shows how the injection capacity increases for various placements of production well. It was also noticed that the effect of having production wells is significantly greater if you have placed them at the center when compared to near the boundary as seen in case of 17 wells (refer to Figure 4.16). This is because the maximum pressure build up is at the center.

Thus, it was concluded that by placement of production well can increase the injection capacity of reservoir but not to a very large extent. Also, using production wells as relief wells are not a very practical viable option, as the produced brine solution is envi-

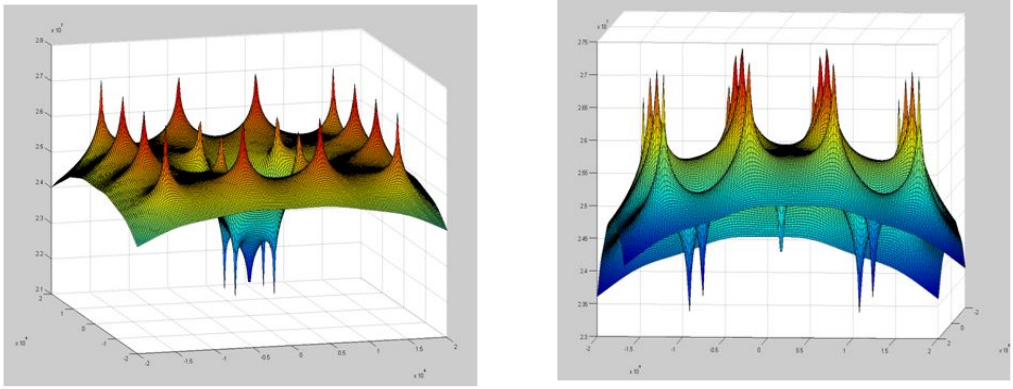

(a) Production wells placed close to center. (b) Production wells placed close to boundary.

Figure 4.16: Well placement for 17 injection wells and 5 production well.

ronmentally non-friendly and leads to an added waste product which needs to be treated and disposed.

4.4 Summary

In this chapter, we have gone through various case scenarios for single well and multiple well modeling which are presently in action where numerical simulations were used for modeling of pressure build-up during CO_2 injection in saline formations. The need of analytical modeling arises in problems during multiple modeling as numerical simulations can be time consuming and complex process. In order to compare or benchmark the applicability of these analytical model during multiple well modeling, the analytical and numerical model for predicting reservoir pressure were compared. Consequently, it was shown that the analytical model for multiple well scenarios are in complete agreement with numerical simulations implying that analytical model is valid and can be further optimized to increase the injection capacity.

In Section 4.3 we demonstrated how CO_2 injection capacity can be increased significantly by increasing the number of wells, optimizing well placement, flow rates and also by using relief wells to ease the pressure inside the reservoir due to CO_2 injection. As we mainly focused on saline aquifers the pressure in the ease can be decreased by placement of brine production well.

Chapter 5

Conclusion

As the world population is growing so is the global energy demand. Thus, to meet this rise in demand, we will need a diverse, reliable and affordable fuel mix so as to enable the economic growth and societal advancements. We can achieve this partly by using technologies like CCS but to make CCS a viable option to reduce carbon footprint, we have to look at ways to increase the injection capacity by screening potential reservoir sites based upon its injection capacity for CO_2 sequestration.

As a first step, we entailed the development of analytical model for prediction of reservoir pressure during CO_2 sequestration in saline aquifer for multiple well scenarios. The analytical model was validated using numerical simulator. These approaches provide information on the sensitivity of numerical simulations to the specific parameters. It was noted that developed analytical model is not aiming to replace numerical simulator but rather to be used for fast preliminary estimates and to optimize the process. Furthermore, the analytical model was also applied to four reservoir field examples for the validation purpose and has been compared with numerical simulations to get good agreement in pressure behavior inside the reservoir.

After modeling, we demonstrated that it can also be used for performing optimization to maximize the injection capacity. The optimization methodology helps to predict the maximum amount of CO_2 that can be injected based on number of wells and the cost associated with each well. We also showed how CO_2 injection capacity can be increased significantly by increasing the number of wells, varying injection cyclic time and injection flow-rate. In addition, we demonstrated that the optimized model using brine production well can decrease the pressure build-up near the injection well and can quite increase the sequestration capacity in saline formations.

5.1 Future work

The methodology used in this work is quite general and it needs further investigation. The following areas are suggested for future work:

1. The proposed analytical model for predicting the pressure is for vertical wells. Further studies can be performed to investigate the BHP of CO_2 in saline formations for horizontal wells which are currently in practice.

2. Creating optimization algorithms using proposed approach. The algorithms should allow handling large number of possible realizations which are function on number of wells, their placement and flow rates of injection.

3. Identifying design patterns which increase storage capacity, and how these patterns depend on particular reservoir properties.

References

[1] Bert Metz. *Carbon dioxide capture and storage: Special report of the Intergovernmental Panel on Climate Change(IPCC)*. Cambridge University Press, 2005.

[2] Sally M Benson and Terry Surles. Carbon dioxide capture and storage: An overview with emphasis on capture and storage in deep geological formations. *Proceedings of the IEEE*, 94(10):1795–1805, 2006.

[3] Howard J Herzog. Scaling up carbon dioxide capture and storage: From megatons to gigatons. *Energy Economics*, 33(4):597–604, 2011.

[4] Yamama Raza. *Uncertainty analysis of capacity estimates and leakage potential for geologic storage of carbon dioxide in saline aquifers*. PhD thesis, Massachusetts Institute of Technology, 2009.

[5] Howard J Herzog. Peer reviewed: what future for carbon capture and sequestration? *Environmental science & technology*, 35(7):148A–153A, 2001.

[6] David W Keith. Towards a strategy for implementing co 2 capture and storage in canada. 2002.

[7] Rattan Lal. Carbon sequestration. *Philosophical Transactions of the Royal Society B: Biological Sciences*, 363(1492):815–830, 2008.

[8] Franklin M Orr et al. Onshore geologic storage of CO_2. *Science*, 325(5948):1656–1658, 2009.

[9] Cesare Marchetti. On geoengineering and the CO_2 problem. *Climatic change*, 1(1):59–68, 1977.

[10] Olav Kaarstad. Emission-free fossil energy from Norway. *Energy Conversion and Management*, 33(5):781–786, 1992.

[11] LGH Van der Meer. Investigations regarding the storage of carbon dioxide in aquifers in the Netherlands. *Energy Conversion and Management*, 33(5):611–618, 1992.

[12] Sam Holloway and Ricks van der Straaten. The joule ii project the underground disposal of carbon dioxide. *Energy Conversion and Management*, 36(69):519–522, 1995. Proceedings of the Second International Conference on Carbon Dioxide Removal.

[13] A Lokhorst and T Wildenborg. Introduction on CO_2 geological storage-classification of storage options. *Oil & gas science and technology*, 60(3):513–515, 2005.

[14] Annual Energy Outlook. Energy information administration. *Department of Energy*, 2002.

[15] CCS Global. Institute (2011). *The global status of CCS*, 2011.

[16] K Michael, G Allinson, A Golab, S Sharma, and V Shulakova. CO_2 storage in saline aquifers-experience from existing storage operations. *Energy Procedia*, 1(1):1973–1980, 2009.

[17] Karsten Michael, Alexandra Golab, Valeriya Shulakova, Jonathan Ennis-King, Guy Allinson, Sandeep Sharma, and Toby Aiken. Geological storage of CO_2 in saline aquifersa review of the experience from existing storage operations. *International Journal of Greenhouse Gas Control*, 4(4):659–667, 2010.

[18] Stefan Bachu. Screening and ranking of sedimentary basins for sequestration of CO_2 in geological media in response to climate change. *Environmental Geology*, 44(3):277–289, 2003.

[19] Martin L Parry. *Climate Change 2007: impacts, adaptation and vulnerability: contribution of Working Group II to the fourth assessment report of the Intergovernmental Panel on Climate Change*, volume 4. Cambridge University Press, 2007.

[20] Sarah E Gasda, Stefan Bachu, and Michael A Celia. Spatial characterization of the location of potentially leaky wells penetrating a deep saline aquifer in a mature sedimentary basin. *Environmental Geology*, 46(6-7):707–720, 2004.

[21] S Bachu and JJ Adams. Sequestration of CO_2 in geological media in response to climate change: capacity of deep saline aquifers to sequester CO_2 in solution. *Energy Conversion and Management*, 44(20):3151–3175, 2003.

[22] John Bradshaw, Stefan Bachu, Didier Bonijoly, Robert Burruss, Sam Holloway, Niels Peter Christensen, and Odd Magne Mathiassen. CO_2 storage capacity estimation: Issues and development of standards. *International Journal of Greenhouse Gas Control*, 1(1):62–68, 2007.

[23] JG Kaldi and CM Gibson-Poole. Storage capacity estimation, site selection and characterisation for CO_2 storage projects. *Report No: RPT08-1001, CO2CRC, Canberra, ACT, AU*, 2008.

[24] A Lucier, and M Zoback. Assessing the economic feasibility of regional deep saline aquifer CO_2 injection and storage: A geomechanics-based workflow applied to the Rose Run sandstone in Eastern Ohio, USA. 2008.

[25] Quanlin Zhou, Jens T Birkholzer, Chin-Fu Tsang, and Jonny Rutqvist. A method for quick assessment of CO_2 storage capacity in closed and semi-closed saline formations. *International Journal of Greenhouse Gas Control*, 2(4):626–639, 2008.

[26] K Michael, S Varma, E Bekele, B Ciftci, J Hodgkinson, L Langhi, B Harris, C Trefry, and K Wouters. Basin resource management and carbon storage: Part ii. 2013.

[27] Prasad Saripalli and Peter McGrail. Semi-analytical approaches to modeling deep well injection of CO_2 for geological sequestration. *Energy Conversion and Management*, 43(2):185–198, 2002.

[28] Alain C Gringarten et al. From straight lines to deconvolution: The evolution of the state of the art in well test analysis. *SPE Reservoir Evaluation & Engineering*, 11(01):41–62, 2008.

[29] Jan Martin Nordbotten, Michael A Celia, and Stefan Bachu. Analytical solutions for leakage rates through abandoned wells. *Water Resources Research*, 40(4), 2004.

[30] Jan Martin Nordbotten, Michael A Celia, Stefan Bachu, and Helge K Dahle. Semianalytical solution for CO_2 leakage through an abandoned well. *Environmental science & technology*, 39(2):602–611, 2005.

[31] Mark Person, Amlan Banerjee, John Rupp, Cristian Medina, Peter Lichtner, Carl Gable, Rajesh Pawar, Michael Celia, Jennifer McIntosh, and Victor Bense. Assessment of basin-scale hydrologic impacts of CO_2 sequestration, Illinois basin. *International Journal of Greenhouse Gas Control*, 4(5):840–854, 2010.

[32] Simon A Mathias, Paul E Hardisty, Mark R Trudell, and Robert W Zimmerman. Approximate solutions for pressure buildup during CO_2 injection in brine aquifers. *Transport in Porous Media*, 79(2):265–284, 2009.

[33] SE Buckley and MC Leverett. Mechanism of fluid displacement in sands. *Trans. Aime*, 146, 1941.

[34] Jan Martin Nordbotten, Michael A Celia, and Stefan Bachu. Injection and storage of CO_2 in deep saline aquifers: Analytical solution for CO_2 plume evolution during injection. *Transport in Porous media*, 58(3):339–360, 2005.

[35] McMillan Burton, Navanit Kumar, and Steven L Bryant. CO_2 injectivity into brine aquifers: Why relative permeability matters as much as absolute permeability. *Energy Procedia*, 1(1):3091–3098, 2009.

[36] Simon A Mathias, Gerardo J González Martínez de Miguel, Kate E Thatcher, and Robert W Zimmerman. Pressure buildup during CO_2 injection into a closed brine aquifer. *Transport in porous media*, 89(3):383–397, 2011.

[37] Simon A Mathias, Paul E Hardisty, Mark R Trudell, and Robert W Zimmerman. Screening and selection of sites for CO_2 sequestration based on pressure buildup. *International Journal of Greenhouse gas control*, 3(5):577–585, 2009.

[38] Christine Ehlig-Economides and Michael J Economides. Sequestering carbon dioxide in a closed underground volume. *Journal of Petroleum Science and Engineering*, 70(1):123–130, 2010.

[39] Azizi, Yildiray Cinar, et al. Approximate analytical solutions for CO_2 injectivity into saline formations. *SPE Reservoir Evaluation & Engineering*, 16(02):123–133, 2013.

[40] Abhishek Joshi. Investigation of multiple well injections for carbon dioxide sequestration in aquifers. 2014.

[41] Y-S Wu, Karsten Pruess, ZX Chen, et al. Buckley-leverett flow in composite porous media. *SPE Advanced Technology Series*, 1(02):36–42, 1993.

[42] Myeong Hwan Noh, Larry Wayne Lake, Steven Lawrence Bryant, Aura N Araque-Martinez, et al. Implications of coupling fractional flow and geochemistry for CO_2 injection in aquifers. *SPE Reservoir Evaluation & Engineering*, 10(04):406–414, 2007.

[43] Henry J Welge et al. A simplified method for computing oil recovery by gas or water drive. *Journal of Petroleum Technology*, 4(04):91–98, 1952.

[44] EG Woods, AG Comer, et al. Saturation distribution and injection pressure for a radial gas-storage reservoir. *Journal of Petroleum Technology*, 14(12):1–389, 1962.

[45] Arthur T Corey. The interrelation between gas and oil relative permeabilities. *Producers monthly*, 19(1):38–41, 1954.

[46] Mehdi Zeidouni, Mehran Pooladi-Darvish, and David Keith. Analytical solution to evaluate salt precipitation during CO_2 injection in saline aquifers. *International Journal of Greenhouse Gas Control*, 3(5):600–611, 2009.

[47] Jens Birkholzer. Research project on CO_2 geological storage and groundwater resources: water quality effects caused by CO_2 intrusion into shallow groundwater. *Lawrence Berkeley National Laboratory*, 2008.

[48] Karsten Pruess, Julio García, Tony Kovscek, Curt Oldenburg, Jonny Rutqvist, Carl Steefel, and Tianfu Xu. Code intercomparison builds confidence in numerical simulation models for geologic disposal of CO_2. *Energy*, 29(9):1431–1444, 2004.

[49] H Alkan, Y Cinar, and EB Ülker. Impact of capillary pressure, salinity and in situ conditions on CO_2 injection into saline aquifers. *Transport in porous media*, 84(3):799–819, 2010.

[50] Yildiray Cinar, Peter R Neal, William G Allinson, Jacques Sayers, et al. Geoengineering and economic assessment of a potential carbon capture and storage site in southeast Queensland Australia. *SPE Reservoir Evaluation & Engineering*, 12(05):660–670, 2009.

[51] T Marhaendrajana, NJ Kaczorowski, TA Blasingame, et al. Analysis and interpretation of well test performance at Arun field, Indonesia. *SPE*, 56487:3–6, 1999.

[52] J Lin and H Yang. Analysis of well-test data in a multiwell reservoir with water injection. In *Paper SPE 110349 presented at the 2007 SPE Annual Technical Conference and Exhibition, Anaheim, CA, Nov*, pages 11–14, 2007.

[53] Johan Zakrisson, Ingrid Edman, Yildiray Cinar, et al. Multiwell injectivity for CO_2 storage. In *SPE Asia Pacific Oil and Gas Conference and Exhibition*. Society of Petroleum Engineers, 2008.

[54] Seyyed M Ghaderi, David W Keith, and Yuri Leonenko. Feasibility of injecting large volumes of CO_2 into aquifers. *Energy Procedia*, 1(1):3113–3120, 2009.

[55] Mehran Pooladi-Darvish, Samane Moghdam, and Don Xu. Multiwell injectivity for storage of CO_2 in aquifers. *Energy Procedia*, 4:4252–4259, 2011.

[56] Hamid. Superposition method used for treating oilfield interference in Iranian water-drive reservoir. *Petroleum Society of Canada*, 2003.

[57] Roland N Horne. Modern well test analysis. *Petroway Inc*, 1995.

[58] Tarek Ahmed et al. *Reservoir engineering handbook*. Gulf Professional Publishing, 2006.

[59] Brant Bennion, Stefan Bachu, et al. Drainage and imbibition relative permeability relationships for supercritical CO_2/brine and H_2S/brine systems in intergranular sandstone carbonate shale and anhydrite rocks. *SPE Reservoir Evaluation & Engineering*, 11(03):487–496, 2008.

[60] Joel Sminchak, Neeraj Gupta, and Jacqueline Gerst. Well test results and reservoir performance for a carbon dioxide injection test in the bass islands dolomite in the Michigan basin. *Environmental Geosciences*, 16(3):153–162, 2009.

[61] Karsten Michael, Stefan Bachu, Beate E Buschkuehle, Kristine Haug, and Stephen Talman. Comprehensive characterization of a potential site for CO_2 geological storage in Central Alberta, Canada. 2009.

[62] Jens T Birkholzer and Quanlin Zhou. Basin-scale hydrogeologic impacts of CO_2 storage: Capacity and regulatory implications. *International Journal of Greenhouse Gas Control*, 3(6):745–756, 2009.

[63] Faye Liu, Peng Lu, Chen Zhu, and Yitian Xiao. Coupled reactive flow and transport modeling of CO_2 sequestration in the Mt. Simon sandstone formation, midwest USA. *International Journal of Greenhouse Gas Control*, 5(2):294–307, 2011.

[64] Samuel Krevor, Ronny Pini, Lin Zuo, and Sally M Benson. Relative permeability and trapping of CO_2 and water in sandstone rocks at reservoir conditions. *Water resources research*, 48(2), 2012.

[65] Ozgur Senel, Nikita Chugunov, et al. CO_2 injection in a saline formation: How do additional data change uncertainties in our reservoir simulation predictions? In *Carbon Management Technology Conference*. Carbon Management Technology Conference, 2012.

[66] Quanlin Zhou, Jens T Birkholzer, Edward Mehnert, Yu-Feng Lin, and Keni Zhang. Modeling basin-and plume-scale processes of CO_2 storage for full-scale deployment. *Groundwater*, 48(4):494–514, 2010.

[67] RA Chadwick, R Arts, and O Eiken. 4d seismic quantification of a growing CO_2 plume at Sleipner, North Sea. In *Geological Society, London, Petroleum Geology Conference series*, volume 6, pages 1385–1399. Geological Society of London, 2005.

[68] Thomas A Buscheck, Yunwei Sun, Mingjie Chen, Yue Hao, Thomas J Wolery, William L Bourcier, Benjamin Court, Michael A Celia, S Julio Friedmann, and Roger D Aines. Active CO_2 reservoir management for carbon storage: Analysis of operational strategies to relieve pressure buildup and improve injectivity. *International Journal of Greenhouse Gas Control*, 6:230–245, 2012.

[69] Annual Energy Outlook. Energy information administration. *Department of Energy*, 2010.

[70] Mahmut Sengul et al. CO_2 sequestration-a safe transition technology. In *SPE International Health Safety & Environment Conference*. Society of Petroleum Engineers, 2006.

[71] DN Espinoza, SH Kim, and JC Santamarina. CO_2 geological storage geotechnical implications. *KSCE Journal of Civil Engineering*, 15(4):707–719, 2011.

[72] S Julio Friedmann. Geological carbon dioxide sequestration. *Elements*, 3(3):179–184, 2007.

[73] Stefan Bachu. CO_2 storage in geological media: Role, means, status and barriers to deployment. *Progress in Energy and Combustion Science*, 34(2):254–273, 2008.

[74] Stefan Bachu. Sequestration of CO_2 in geological media in response to climate change: road map for site selection using the transform of the geological space into the CO_2 phase space. *Energy Conversion and management*, 43(1):87–102, 2002.

[75] Mike J Bickle. Geological carbon storage. *Nature Geoscience*, 2(12):815–818, 2009.

[76] JCM Pires, FG Martins, MCM Alvim-Ferraz, and M Simões. Recent developments on carbon capture and storage: An overview. *Chemical Engineering Research and Design*, 89(9):1446–1460, 2011.

[77] Burton McMillan, Navanit Kumar, Steven Lawrence Bryant, et al. Time-dependent injectivity during CO_2 storage in aquifers. In *SPE Symposium on Improved Oil Recovery*. Society of Petroleum Engineers, 2008.

[78] Steven Chu and Arun Majumdar. Opportunities and challenges for a sustainable energy future. *Nature*, 488(7411):294–303, 2012.

[79] Laurie P Dake. *The practice of reservoir engineering (revised edition)*. Elsevier, 2001.

[80] Jean-Philippe Nicot. Evaluation of large-scale CO_2 storage on fresh-water sections of aquifers: An example from the Texas Gulf coast basin. *International Journal of Greenhouse Gas Control*, 2(4):582–593, 2008.

[81] Stephen Pacala and Robert Socolow. Stabilization wedges: solving the climate problem for the next 50 years with current technologies. *Science*, 305(5686):968–972, 2004.

[82] Jean-Philippe Nicot, Seyyed A Hosseini, and Silvia V Solano. Are single-phase flow numerical models sufficient to estimate pressure distribution in CO_2 sequestration projects? *Energy Procedia*, 4:3919–3926, 2011.